Available online at www.sciencedirect.com
ScienceDirect
ELSEVIER
Palaeogeography, Palaeoclimatology, Palaeoecology 254 (2007) 194–216
PALAEO
www.elsevier.com/locate/palaeo

Trace element chemostratigraphy of two Ediacaran–Cambrian successions in South China: Implications for organosedimentary metal enrichment and silicification in the early Cambrian

Qingjun Guo [a,b,*], Graham A. Shields [b,c], Congqiang Liu [a], Harald Strauss [b], Maoyan Zhu [d], Daohui Pi [a], Tatiana Goldberg [b,c], Xinglian Yang [e]

[a] State Key Laboratory of Environmental Geochemistry, Institute of Geochemistry, Chinese Academy of Sciences, Guiyang 550002, China
[b] Geologisch-Paläontologisches Institut, Westfälische Wilhelms-Universität Münster, Corrensstrasse 24, 48149 Münster, Germany
[c] School of Earth Sciences, James Cook University, Townsville, Queensland 4811, Australia
[d] Nanjing Institute of Geology and Palaeontology, Chinese Academy of Sciences, Nanjing 210008, China
[e] College of Resource and Environment of Guizhou University, Guiyang 550003, China

Accepted 5 March 2007

Abstract

A trace element study is presented of two Ediacaran–Early Cambrian sedimentary successions in South China: the Shatan section, Sichuan Province, which represents a shallow platform setting, and the Songtao section, Guizhou Province, which corresponds to a more basinal, depositional environment. Across South China, sedimentary strata of this age exhibit characteristic trace metal enrichments in generally organic-rich, stratigraphically correlative, transgressive units. Trace element (including REE) data are used here to determine the palaeoenvironmental and diagenetic conditions during this Early Cambrian interval of metal scavenging that resulted in enrichments over grey shale of Mo > Cd > V > U > Ni > Ag > Zn > Cu > Pb. At Shatan, high organic carbon contents (up to 5% TOC) correlate with Mo enrichment, which indicates that metal scavenging was linked to organic productivity and decay. Low Th/U ratios are consistent with highly reducing conditions during metal scavenging, while extremely high V contents imply that bottom waters were possibly euxinic at times of extreme anoxia. At Songtao, very low Th/U ratios are strongly associated with high V/Sc and low $\delta^{13}C_{org}$, implying that anoxia, organic decomposition and metal sequestration were associated in the deepwater facies, too. There is no unambiguous trace element evidence that hydrothermal activity contributed to metal enrichment in South China during the Early Cambrian. The systematic relationship with ocean transgression suggests that enrichment was caused largely by oceanographic changes to organic productivity and burial rather than post-depositional fluid flow. Negative Ce anomalies and seawater-like REE distribution patterns are a feature of the Liuchapo chert and lower black shales of the Jiumenchong Formation at Songtao. Ce depletion indicates that authigenic components of these sedimentary units formed under oxic conditions, which contradicts the other geochemical redox proxies. We argue that this chert derived primarily from biogenic silica from siliceous plankton, which formed above a redox boundary within the water column. Neither silicification nor hydrothermal fluids, contrary to some published models, played a significant role in metal transport.

Keywords: Ediacaran; Cambrian; Rare earth elements; Trace elements; Paleoredox proxies; Yangtze Platform; South China; Black shales

* Corresponding author. State Key Laboratory of Environmental Geochemistry, Institute of Geochemistry, Chinese Academy of Sciences, Guiyang 550002, China. Tel.: +86 851 5891375; fax: +86 851 5891721.
E-mail address: guoqingjun@vip.skleg.cn (Q. Guo).

0031-0182/$ - see front matter © 2007 Elsevier B.V. All rights reserved.
doi:10.1016/j.palaeo.2007.03.016

1. Introduction

China's Yangtze Platform contains a sedimentary succession of Ediacaran and Early Cambrian age, with different paleoenvironmental settings including inner shelf, outer shelf, slope and basin deposits (Fig. 1). These are well exposed in several sections across a transect from platform to basin that offers an opportunity to study the marine paleoenvironment during this critical interval in Earth history. Resting on glaciogenic rocks of the Nantuo Formation, the sedimentary succession comprises, in ascending stratigraphic order: calcareous sediments, cherts, black shales, and phosphorites of the Sinian Doushantuo and Dengying (time equivalent of the Liuchapo Formation) Formations and black shales of the Early Cambrian Niutitang Formation (time equivalent of the Guojiaba and the Jiumenchong Formations) (Fig. 2) (Guo et al., 2007-this volume). The Niutitang Formation is characterized by anomalous enrichments of many transition and other metals.

Metal enrichment is a feature of all organic-rich shales (black shales), which are a characteristic feature of warm intervals in Earth history, e.g. the Cambrian, late Devonian–Carboniferous, mid-late Permian and Cretaceous Periods. Because of the systematic association between metal enrichment and black shales, it seems likely that anoxia caused by organic productivity and decay played the major role in most metal enrichment. However, there are many long-lasting debates about whether metals in particular black shale units were sequestered primarily from anoxic seawater and pore waters or whether they were supplied by hydrothermal fluids (e.g. Mao et al., 2002; Cruse and Lyons, 2004). Recently, several studies have used a range of trace element and isotopic proxies to determine the conditions under which black shales scavenged transition metals.

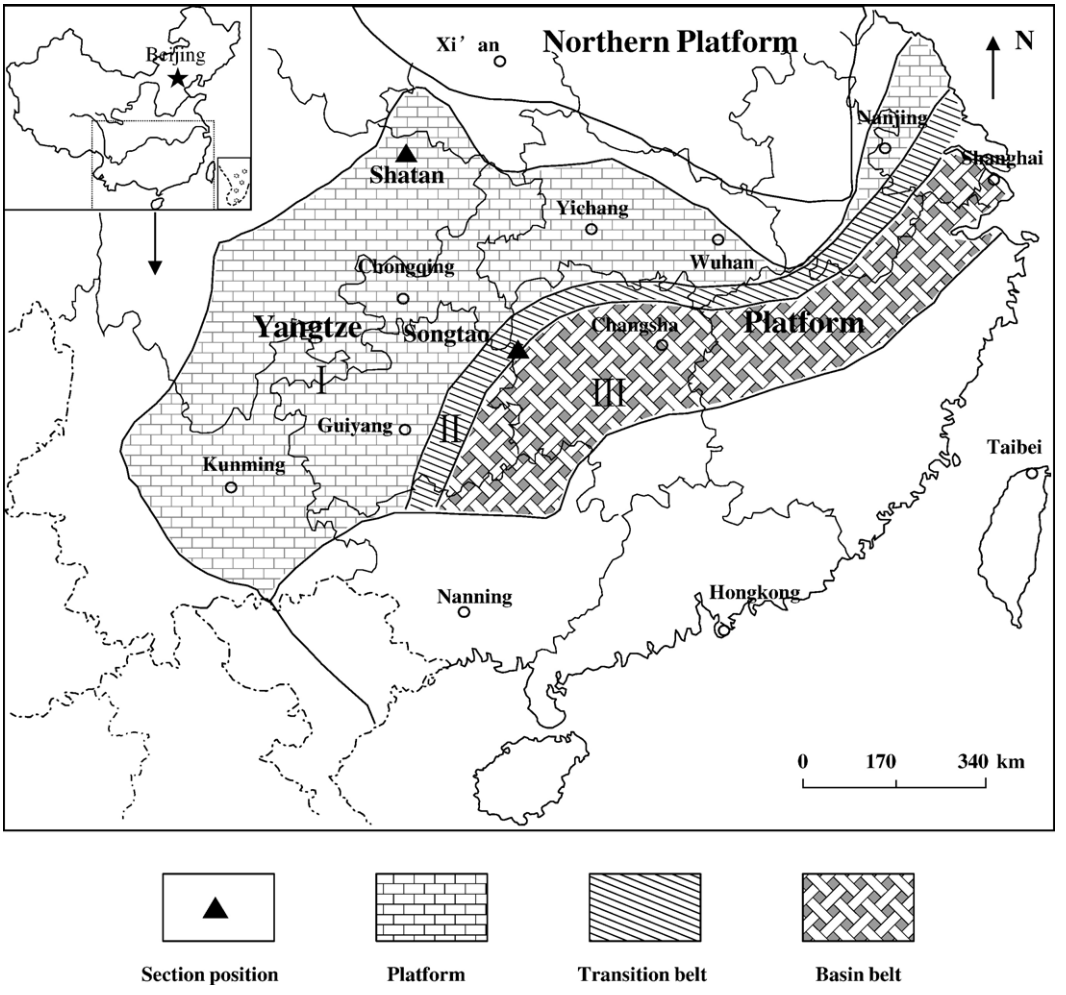

Fig. 1. Map showing the locations and depositional environments of the studied sections of the Yangtze Platform, South China (modified after Steiner et al., 2001).

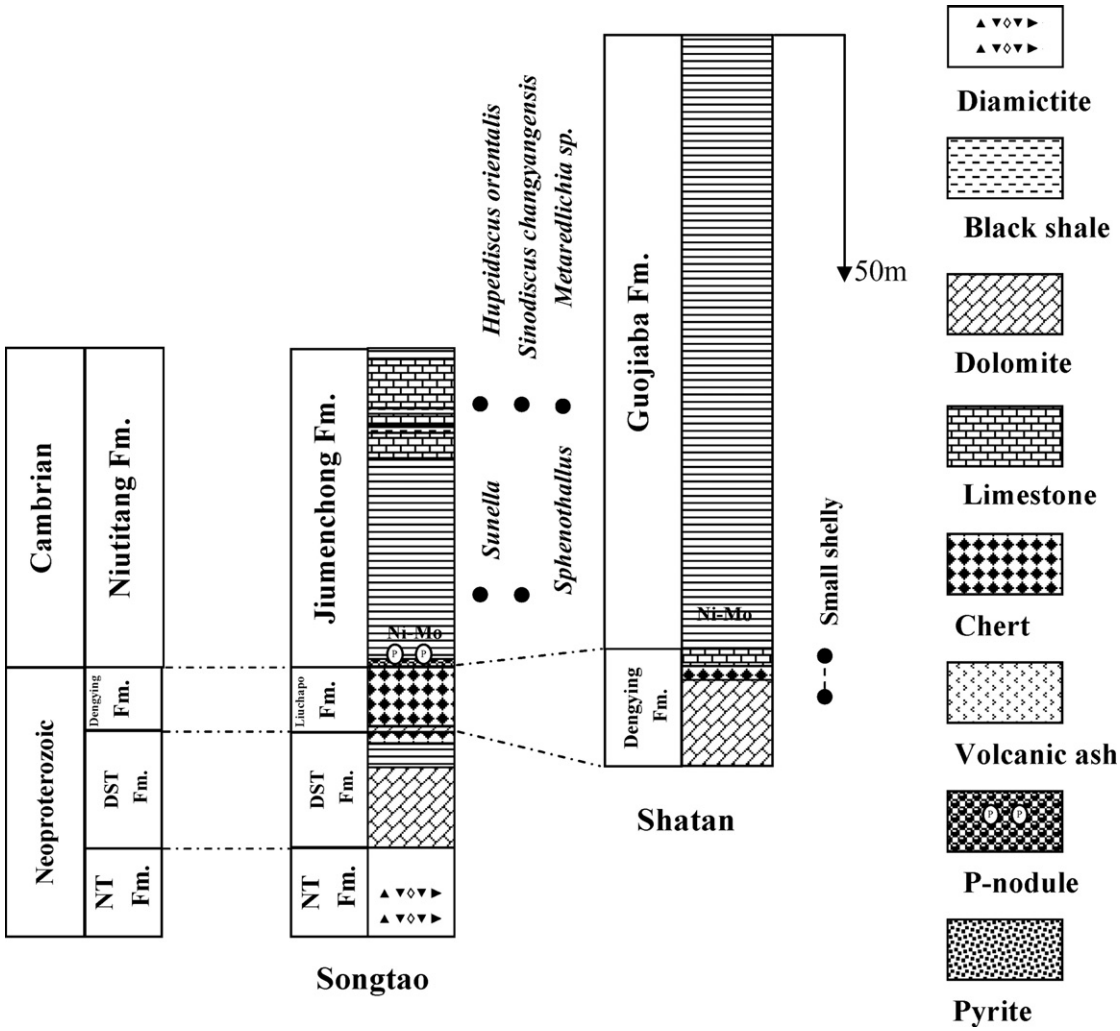

Fig. 2. Lithological profiles of Songtao section, Shatan section and their proposed correlation.

In this paper, we report the results of a comprehensive geochemical study into Early Cambrian black shales of the Yangtze Platform as a contribution to this debate.

Published REE and trace element studies of the Early Cambrian of South China (e.g. Shields and Stille, 2001; Steiner et al., 2001; Chen et al., 2003; Pan et al., 2004; Li and Gao, 1995, 1996) only reported elemental data for either the Yangtze carbonate platform or the basin belt but not both as in the present study. Here we present trace element, including REE, geochemical data through the post-glacial Sinian and Early Cambrian stratigraphy along a transect across the different facies represented in the Shatan and Songtao sections. We apply an unusually wide range of proposed paleoenvironmental and paleo-redox proxies, such as Th/U, V/Cr, V/Sc, V/(V+Ni), Mo, Ce anomalies, and C- and S-isotopes, in order to determine the origins of sequestered metals and silicification in these different settings. Our data suggest that metal enrichment was achieved through scavenging as metal sulphides during periods of bottom water anoxia, and rarely euxinia, caused by high organic flux to the sediment (cf. Mao et al., 2002). We conclude, in agreement with Braun et al. (2003), that biogenic silica is likely to be the primary contributor of silica to cherts and siliceous black shale in deeper water facies of the Yangtze Platform.

2. Geological setting and sections

A conformable succession of lithologically diverse marine sediments was deposited on the Yangtze Platform, South China during the Precambrian–Cambrian

transitional period (Zhu et al., 2003). Well preserved rocks document a series of different geological features including sea-level fluctuations, ocean anoxia, phosphorite deposition and the Cambrian bio-radiation (Guo et al., 2003). We studied this sequence of sedimentary rocks at the following locations: the Shatan section (carbonate platform, shelf of northern Yangtze Platform), Nanjiang County, Sichuan Province, and the Songtao section (a slope to basinal setting, Yangtze Platform), Songtao County, Guizhou Province (Fig. 1).

The Shatan section straddles the Precambrian–Cambrian boundary. It comprises the upper part of the Ediacaran (Neoproterozoic) Dengying Formation and the lower part of the Guojiaba Formation (Fig. 2), representing a shallow shelf, depositional environment (Fig. 1). Lithologies include light grey carbonates, black shale and siliceous rocks, with abundant small-shelly fossils (SSF) preserved in the Kuanchanpu Member of the lowermost Guojiaba Formation (equivalent to the Niutitang Formation) (Steiner et al., 2004). Fossils belong to the first two SSF Assemblages of the Cambrian in South China (*Anabarites trisulcatus–Protohertzina anabarica* and *Paragloborilus subglobosus–Purella squamulosa*) and are abundant in the upper half of the Kuanchanpu Formation, especially in the phosphorite breccia level, which implies a Nemakit–Daldynian age (Steiner et al., 2004; Goldberg et al., 2007-this volume) (Fig. 2). The biostratigraphy of the Shatan section has been studied in detail (Yang et al., 1983; Yang and He, 1984; He and Yang, 1986; Steiner et al., 2004).

On the Yangtze Platform, a transitional belt is situated between the carbonate platform and the basinal belt. The Songtao section is located in a slope to basinal setting and comprises the Doushantuo, Liuchapo and Jiumenchong Formations (Fig. 2), all representing slope deposition (Fig. 1). The major lithofacies of the Doushantuo Formation comprises bedded, micritic carbonates, and finely laminated black shales. The upper Sinian Liuchapo Formation (equivalent to the Dengying Formation) consists of black siliceous rocks, phosphatic–siliceous shale and minor limestone concretions. The Jiumenchong Formation (equivalent to the Niutitang Formation) consists of black–greyish carbonaceous shale, limestone and mudstone. The lowermost part of this unit is composed of nodular phosphate rocks. In the black shales of the lower part of the Jiumenchong Fm., bivalved arthropods (*Sunella*) and tubular fossils (*Sphenothallus*) have been reported (at 15 m above the base of the formation) while the upper part consists of limestone with trilobites, including *Hupeidiscus orientalis*, *Sinodiscus changyangensis* and *Metaredlichia* sp. (Yang et al., 2003) (Fig. 2).

U–Pb zircon dates from volcanic ash beds within the Doushantuo Formation (China) indicate that its deposition occurred between 635 and 551 million years ago (Condon et al., 2005). The age of the Precambrian–Cambrian boundary has been dated elsewhere at 544 Ma (Bowring et al., 1993), respectively is placed at 542 Ma (Gradstein et al., 2005). Mao et al. (2002) reported Re–Os isotopic compositions, which yield an isochron age of 541±16 Ma for Lower Cambrian Ni–Mo sulphide ores of South China.

3. Samples and analytical methods

A total of 79 samples (Tables 1 and 2) were analysed, from basal Sinian (Ediacaran) post-glacial cap carbonates at the base of the Doushantuo Formation through the largely cherty Liuchapo Formation or carbonate-rich Dengying Formation to black shales of the Early Cambrian Guojiaba and Jiumenchong Formations (equivalent to the Niutitang Formation). Stratigraphic positions for the samples are provided in Figs. 2–4 and Tables 1 and 2.

Prior to geochemical analyses, all fresh samples were chipped and pulverized (200 mesh). Powdered rock samples were leached with 2N HCl in order to remove carbonate and calcium phosphate minerals, after which the residues were fully digested using a mixture of HF and HNO_3. After evaporation, samples were redissolved in 1N HNO_3 for ICP-MS analysis at the key laboratory of ore deposit geochemistry, Institute of Geochemistry, Chinese Academy of Sciences, Guiyang, China. All data relate to HCl-insoluble residues. All element ratios presented in tables and figures are weight ratios. Analytical precision for elemental concentrations was generally better than 5%. Eu/Eu*, Ce/Ce* and Y/Y* were calculated using published formulae (Bau and Dulski, 1996), and have been normalized against PAAS (Mclennan, 1989):

$$\mathrm{Eu/Eu^*} = \mathrm{Eu_{PAAS}} \Big/ \left(\frac{1}{2}\mathrm{Sm_{PAAS}} + \frac{1}{2}\mathrm{Gd_{PAAS}}\right)$$

$$\mathrm{Ce/Ce^*} = \mathrm{Ce_{PAAS}} \Big/ \left(\frac{1}{2}\mathrm{La_{PAAS}} + \frac{1}{2}\mathrm{Pr_{PAAS}}\right)$$

$$\mathrm{Y/Y^*} = \mathrm{Y_{PAAS}} \Big/ \left(\frac{1}{2}\mathrm{Dy_{PAAS}} + \frac{1}{2}\mathrm{Ho_{PAAS}}\right)$$

$$\mathrm{Pr/Pr^*} = \mathrm{Pr_{PAAS}} \Big/ \left(\frac{1}{2}\mathrm{Ce_{PAAS}} + \frac{1}{2}\mathrm{Nd_{PAAS}}\right).$$

Table 1
REE (ppm) and trace element concentrations in the acid-insoluble fractions of sedimentary rocks from the Shatan section, Sichuan Province, South China

Fig. 1-1

Sample	Unit	Lithology	Depth(m)	La	Ce	Pr	Nd	Sm	Eu	Gd	Tb	Dy	Ho	Er	Tm	Yb	Lu	Y	Sc	Ti
Sat531	Guojiaba Fm.	Black shale	154.1	28.19	54.44	6.38	25.42	4.64	1.15	4.61	0.65	3.95	0.80	2.27	0.34	2.14	0.31	22.13	10.30	3047.90
Sat530	Guojiaba Fm.	Black shale	131.5	29.92	58.93	6.90	28.24	5.23	1.00	4.86	0.71	4.04	0.88	2.49	0.36	2.42	0.39	23.80	11.42	3580.84
Sat529	Guojiaba Fm.	Black shale	124.5	29.95	56.71	6.66	25.90	4.88	1.01	4.58	0.76	4.28	0.87	2.52	0.37	2.64	0.39	23.53	10.60	3383.23
Sat528	Guojiaba Fm.	Black shale	118.5	32.12	59.63	6.82	26.51	4.96	1.02	4.52	0.68	3.97	0.80	2.51	0.36	2.27	0.35	21.55	13.34	4239.52
Sat527	Guojiaba Fm.	Black shale	113.5	29.32	57.32	6.89	28.05	5.58	1.07	4.90	0.77	4.55	0.94	2.64	0.38	2.57	0.40	24.79	12.39	4059.88
Sat526	Guojiaba Fm.	Black shale	109	34.09	65.78	7.89	31.54	5.61	1.14	5.64	0.82	4.94	1.05	2.99	0.49	3.00	0.43	27.41	13.65	3802.40
Sat525	Guojiaba Fm.	Black shale	102.4	30.90	59.34	7.09	28.29	5.05	1.06	4.93	0.73	4.11	0.94	2.57	0.39	2.57	0.40	23.38	12.07	3838.32
Sat524	Guojiaba Fm.	Black shale	99.4	33.21	63.54	7.33	29.02	5.69	1.11	5.27	0.76	4.66	0.94	2.74	0.41	2.87	0.43	25.40	11.70	3652.69
Sat523	Guojiaba Fm.	Black shale	93.5	29.29	56.25	6.69	26.28	5.04	1.03	4.87	0.76	4.29	0.85	2.27	0.37	2.34	0.34	23.29	10.55	3431.14
Sat522	Guojiaba Fm.	Black shale	90	39.76	74.17	8.64	32.47	6.16	1.18	5.89	0.84	4.84	0.96	2.91	0.42	2.92	0.44	25.07	14.05	4215.57
Sat521	Guojiaba Fm.	Black shale	86.1	35.96	69.63	8.34	32.71	6.32	1.21	6.15	0.83	5.23	1.09	3.11	0.47	3.01	0.44	27.89	14.32	4508.98
Sat520	Guojiaba Fm.	Black shale	80.8	33.56	64.37	7.51	30.52	5.65	1.16	5.55	0.78	4.81	0.95	2.57	0.41	2.65	0.38	24.98	12.82	4143.71
Sat519	Guojiaba Fm.	Black shale	76.5	34.40	65.59	7.52	30.66	5.32	1.14	5.80	0.79	4.58	0.94	2.69	0.42	2.72	0.43	25.41	13.85	4173.65
Sat518	Guojiaba Fm.	Black shale	70.7	33.09	63.77	7.51	30.60	5.64	1.30	5.60	0.81	4.55	0.95	2.77	0.43	2.72	0.41	25.21	11.99	4125.75
Sat517	Guojiaba Fm.	Black shale	67.1	36.12	69.43	8.27	32.70	6.28	1.31	6.00	0.80	4.66	1.04	2.82	0.44	2.61	0.41	25.76	14.36	4407.19
Sat516	Guojiaba Fm.	Black shale	61.5	35.57	66.86	8.01	31.86	6.21	1.30	5.70	0.77	4.63	1.04	2.94	0.47	3.00	0.42	27.65	15.26	4389.22
Sat515	Guojiaba Fm.	Black shale	56.3	42.80	78.56	9.16	36.19	7.08	1.57	6.88	0.94	5.44	1.14	3.38	0.50	3.09	0.46	31.66	15.39	5095.81
Sat514	Guojiaba Fm.	Black shale	53.5	16.06	33.00	4.65	22.24	10.10	2.57	7.84	1.18	6.84	1.36	3.74	0.47	3.56	0.47	43.79	9.04	1245.51
Sat513	Guojiaba Fm.	Black shale	50.9	40.36	74.51	9.10	35.58	6.63	1.29	6.31	0.88	4.71	1.02	3.03	0.44	2.88	0.39	26.79	16.15	4335.33
Sat512	Guojiaba Fm.	Black shale	46.4	38.63	71.14	8.47	37.49	6.16	1.19	6.00	0.81	3.88	1.44	2.47	0.92	3.74	0.40	25.91	15.29	4113.77
Sat511	Guojiaba Fm.	Black shale	42.4	28.64	53.97	6.66	26.38	5.34	1.07	4.89	0.72	4.25	0.83	2.45	0.37	2.42	0.33	24.68	12.84	3497.01
Sat510	Guojiaba Fm.	Black shale	38.4	29.99	56.11	6.94	28.23	5.59	1.14	5.49	0.82	4.61	1.04	2.79	0.42	2.68	0.40	27.63	13.05	3401.20
Sat509	Guojiaba Fm.	Black shale	36.4	27.05	50.42	6.16	24.82	4.82	1.06	4.87	0.72	4.14	0.90	2.66	0.38	2.46	0.37	25.31	12.54	3730.54
Sat508	Guojiaba Fm.	Black shale	34	33.86	60.88	7.48	30.84	5.70	1.19	5.48	0.76	4.61	0.93	2.76	0.41	2.75	0.38	27.74	13.30	3598.80
Sat507	Guojiaba Fm.	Black shale	32	33.80	59.29	7.19	29.03	5.85	1.21	5.40	0.85	4.87	0.94	2.73	0.43	2.64	0.39	28.69	13.40	3814.37
Sat506	Guojiaba Fm.	Black shale	30	34.29	63.20	7.61	30.73	5.74	1.09	5.81	0.79	4.85	1.00	2.69	0.43	2.91	0.47	28.65	14.45	4305.39
Sat505	Guojiaba Fm.	Black shale	28.7	31.25	57.18	6.99	26.73	5.00	1.23	5.26	0.75	4.34	0.95	2.94	0.43	2.65	0.39	26.49	15.03	3994.01
Sat504	Guojiaba Fm.	Black shale	27.6	30.02	54.08	6.57	26.45	4.76	1.10	4.88	0.70	4.34	0.87	2.56	0.39	2.54	0.35	24.77	16.21	4053.89
Sat503	Guojiaba Fm.	Black shale	26.8	37.85	67.39	8.27	31.14	5.83	1.12	5.36	0.75	4.56	0.94	2.94	0.42	2.73	0.41	25.55	16.45	4047.90
Sat502	Guojiaba Fm.	Black shale	25.8	37.35	68.63	8.35	34.95	6.88	1.46	6.86	0.98	5.55	1.19	3.48	0.51	3.26	0.47	31.24	18.52	4335.33
Sat501	Guojiaba Fm.	Black shale	25.25	37.04	58.66	5.73	19.16	2.42	0.57	2.32	0.35	2.11	0.50	1.61	0.25	1.88	0.32	13.26	16.33	4449.10
Sat500	Guojiaba Fm.	Black shale	25.05	9.74	12.98	2.00	9.63	2.26	0.59	3.06	0.37	1.85	0.40	0.90	0.11	0.56	0.08	16.37	3.86	311.38
Sat533	Dengying Fm.	Limestone	24.55	0.57	0.71	0.10	0.53	0.18	0.02	0.17	0.02	0.15	0.03	0.09	0.01	0.04	0.01	1.51	2.71	11.98
Sat534	Dengying Fm.	Limestone	23.55	0.67	0.80	0.13	0.79	0.20	0.06	0.29	0.03	0.25	0.04	0.13	0.02	0.09	0.01	2.46	3.46	11.98
Sat535	Dengying Fm.	Limestone	21.95	4.93	8.58	1.09	4.17	0.81	0.15	0.71	0.12	0.55	0.13	0.38	0.05	0.29	0.03	3.98	4.04	299.40
Sat536	Dengying Fm.	Limestone	20.45	2.64	4.57	0.44	1.84	0.33	0.11	0.34	0.04	0.20	0.05	0.18	0.02	0.12	0.02	1.78	4.05	113.77
Sat537	Dengying Fm.	dolomite	18.85	2.58	3.62	0.48	1.99	0.40	0.06	0.33	0.06	0.30	0.05	0.14	0.03	0.14	0.02	2.36	4.23	131.74
Sat538	Dengying Fm.	Dolomite	18.65	1.67	2.39	0.30	1.25	0.22	0.07	0.25	0.04	0.25	0.06	0.18	0.02	0.13	0.02	2.15	4.16	113.77
Sat539	Dengying Fm.	Dolomite	17.85	0.47	0.65	0.12	0.52	0.38	0.11	0.21	0.04	0.18	0.04	0.12	0.04	0.09	0.03	0.92	3.95	5.99
Sat540	Dengying Fm.	Dolomite	16.05	0.19	0.34	0.03	0.15	0.04	0.02	0.01	0.00	0.02	0.00	0.01	0.00	0.01	0.00	0.09	4.36	0.00
Sat541	Dengying Fm.	Dolomite	13.65																4.31	0.00
Sat542	Dengying Fm.	Dolomite	10.85																4.42	5.99
Sat543	Dengying Fm.	Dolomite	9.35																3.98	0.00
Sat544	Dengying Fm.	Dolomite	7.05	0.12	0.22	0.02	0.11	0.02	0.01	0.01	0.00	0.01	0.00	0.01	0.00	0.00	0.00	0.11	3.82	0.00
Sat545	Dengying Fm.	Dolomite	3.3	0.14	0.30	0.03	0.21	0.06	0.02	0.04	0.01	0.03	0.01	0.01	0.00	0.01	0.00	0.15	4.06	0.00
Sat546	Dengying Fm.	Dolomite	0																3.89	0.00
Average shale	(Drever, et al 1988; Mclennan, 2001)																		10.00	
Guojiaba average																			13.27	3791.54
Dengying average																			3.96	49.62
Lower Guojiaba average																			13.95	3689.33
Upper Guojiaba average																			12.49	3907.39

Enrichment factors (Guojiaba Fm.)		1.33
Enrichment factors (upper Guojiaba Fm.)		1.25
Enrichment factors (lower Guojiaba Fm.)		1.39
Enrichment factors (Dengying Fm.)		0.40
Non-hydrothermal sediments		
Hydrothermal sediments	(Li and Gao, 1996)	

Fig. 1-2

Sample	V	Cr	Mn	Ni	Cu	Zn	Ga	Ge	As	Rb	Sr	Zr	Nb	Mo	Ag	Cd	In	Sn	Sb	Cs
Sat531	64.82	56.19	565.89	22.46	9.84	40.94	11.50	0.83	15.78	48.25	466.89	144.75	8.12	0.90	0.14	0.15	0.06	1.63	4.96	1.98
Sat530	77.14	63.68	480.62	28.81	20.87	77.26	13.57	1.25	14.62	79.20	291.16	206.32	9.53	2.85	0.19	0.41	0.06	4.56	5.97	3.62
Sat529	71.52	61.41	426.36	25.21	15.27	42.49	15.00	1.55	10.23	87.67	330.43	172.06	9.87	1.92	0.18	0.19	0.06	2.95	2.26	4.16
Sat528	97.73	84.19	480.62	41.86	20.93	79.76	16.55	1.14	13.98	86.49	301.10	163.50	11.28	1.89	0.21	0.28	0.07	2.44	1.35	3.78
Sat527	83.10	69.97	503.88	29.26	20.93	86.45	15.01	1.40	15.10	82.18	207.35	233.52	10.67	3.85	0.19	0.39	0.06	2.14	2.07	3.52
Sat526	77.63	68.69	403.10	27.06	16.56	62.23	15.31	1.24	13.83	73.71	260.26	233.36	11.10	2.36	0.13	0.28	0.07	2.44	1.44	3.27
Sat525	87.24	73.93	573.64	28.66	21.32	116.97	16.07	1.40	11.88	89.90	200.54	226.39	10.55	4.03	0.28	0.49	0.05	2.61	1.52	3.77
Sat524	82.00	66.40	403.10	35.27	20.67	56.12	16.27	1.49	16.79	88.11	350.60	224.38	10.68	5.09	0.24	0.32	0.06	3.57	1.42	4.35
Sat523	74.97	65.64	449.61	31.14	17.74	50.87	12.25	1.21	13.63	60.26	375.50	202.31	9.03	3.93	0.13	0.21	0.04	2.13	0.96	2.79
Sat522	102.05	84.86	379.84	42.65	23.32	87.25	16.33	1.44	27.16	83.21	308.84	261.91	11.41	5.19	0.22	0.37	0.07	2.59	2.06	3.22
Sat521	103.28	82.35	457.36	40.81	24.21	98.92	16.60	1.15	15.26	82.94	251.52	282.73	11.69	4.55	0.18	0.48	0.07	2.19	6.30	3.40
Sat520	95.25	77.65	542.64	36.69	25.80	89.36	15.86	1.43	14.65	77.42	375.08	203.27	10.42	3.37	0.19	0.35	0.49	2.34	1.15	3.53
Sat519	92.45	82.11	519.38	32.73	24.64	65.21	16.71	1.35	16.09	83.45	261.11	234.65	10.62	5.62	0.25	0.32	0.27	2.44	3.91	3.64
Sat518	85.34	71.07	511.63	30.32	21.05	103.21	14.65	1.40	17.61	73.31	273.67	244.31	10.66	6.77	0.22	0.51	0.06	1.99	1.66	2.92
Sat517	107.45	87.22	519.38	37.62	30.01	75.24	17.04	1.28	19.68	85.76	294.33	223.26	11.43	7.05	0.25	0.33	0.07	2.66	1.45	4.22
Sat516	162.23	95.75	348.84	76.54	40.79	86.41	17.99	1.29	27.06	100.44	126.25	220.48	11.40	18.74	0.33	0.62	0.06	2.80	3.65	4.49
Sat515	484.23	114.35	356.59	131.75	48.16	156.13	21.80	1.43	43.23	125.57	137.00	277.01	13.27	44.19	0.41	1.34	E 0.093	3.19	6.51	5.90
Sat514	229.96	27.10	1085.27	57.75	29.49	169.72	4.55	0.45	33.64	20.35	430.33	62.41	4.28	13.40	0.18	3.54	0.04	0.61	1.95	1.01
Sat513	424.18	91.47	356.59	119.41	45.11	134.80	18.78	1.32	33.70	103.85	130.85	210.51	11.81	36.59	0.50	1.43	0.07	2.54	12.55	4.36
Sat512	406.25	92.38	333.33	116.55	43.65	124.34	18.24	5.67	33.29	99.75	125.78	209.42	11.47	35.88	0.46	1.28	1.01	2.21	12.44	4.34
Sat511	298.00	86.37	302.33	114.78	41.70	85.33	16.98	1.36	23.38	96.92	158.99	167.15	9.38	38.60	0.38	0.83	0.07	4.23	2.32	5.80
Sat510	188.49	86.67	472.87	68.25	49.17	130.42	16.39	1.28	30.09	91.77	208.71	164.06	9.25	70.92	0.41	1.33	0.05	2.26	3.33	5.39
Sat509	1198.18	104.37	302.33	158.19	49.54	159.76	15.55	1.28	38.67	100.65	129.34	173.40	9.89	38.96	0.84	2.16	0.05	2.41	5.27	5.64
Sat508	2141.22	127.84	341.09	144.10	62.91	270.00	17.07	1.24	35.18	105.82	129.24	172.86	9.85	29.91	0.98	5.47	0.07	2.20	8.15	5.41
Sat507	2049.58	164.25	317.83	140.70	63.91	597.53	17.60	1.28	40.88	106.00	132.47	188.58	10.30	25.50	1.32	10.48	0.05	2.40	9.45	5.48
Sat506	444.05	100.82	294.57	122.48	50.79	107.34	18.29	1.13	48.54	106.41	101.94	227.14	12.09	70.20	1.01	1.30	0.06	2.53	5.94	5.64
Sat505	424.06	103.31	441.86	103.37	56.29	184.29	18.92	1.20	46.70	119.77	129.25	179.53	11.41	42.79	0.57	1.94	0.08	2.51	3.73	7.09
Sat504	215.05	103.10	341.09	74.21	38.81	126.45	21.25	1.19	31.84	130.71	110.57	167.47	11.37	12.03	0.29	0.86	0.08	2.64	1.39	8.52
Sat503	187.79	108.60	310.08	54.21	34.20	158.25	20.43	1.24	20.26	130.61	81.41	176.28	11.39	5.44	0.25	0.68	0.07	2.97	4.27	7.80
Sat502	164.43	103.89	255.81	54.35	33.68	146.53	21.32	1.15	19.04	137.31	69.09	187.88	13.20	2.21	0.22	2.29	0.06	2.67	1.98	9.00
Sat501	148.58	103.09	116.28	37.26	45.05	102.16	21.86	1.27	26.82	138.58	87.81	190.07	12.82	4.98	0.25	0.71	0.06	3.69	1.81	8.59
Sat500	43.05	13.19	837.21	12.93	3.18	25.25	2.67	0.14	16.83	7.15	361.96	13.80	1.18	1.06	0.01	0.43	0.02	1.15	1.73	0.31
Sat533	6.79	2.54	240.31	10.29	0.73	0.64	0.13	0.10	23.06	0.34	273.12	1.21	0.05	0.98	0.01	0.22	0.01	1.56	1.10	0.01
Sat534	15.59	6.59	54.26	16.80	2.27	6.82	0.10	0.02	13.56	0.01	206.13	0.68	0.03	0.77	0.02	0.17	0.00	0.12	0.98	0.01
Sat535	22.41	10.65	573.64	15.49	6.89	16.85	1.95	0.12	30.56	9.44	76.43	12.01	1.21	3.32	0.01	0.32	0.01	0.74	2.76	0.79
Sat536	7.33	5.02	1279.07	9.37	2.41	103.44	0.84	0.01	20.71	3.00	134.10	4.63	0.44	1.81	0.02	0.25	0.01	0.51	1.07	0.31
Sat537	11.23	5.84	713.18	9.67	1.58	12.70	0.90	0.02	14.82	3.92	92.18	5.72	0.52	3.02	0.01	0.39	0.00	0.29	2.39	0.33
Sat538	7.59	5.66	565.89	8.40	4.86	26.64	0.67	0.04	20.29	3.22	84.28	4.56	0.48	2.73	0.01	0.27	0.01	0.31	1.62	0.28
Sat539	1.74	94.16	100.78	57.73	0.44	1.39	0.21	0.19	12.16	0.14	56.94	0.75	0.09	0.91	0.08	0.26	0.04	0.41	0.79	0.05
Sat540	3.14	29.56	62.02	17.91	1.47	0.23	0.02	0.04	13.72	0.08	61.90	0.35	0.04	0.28	0.00	0.14	0.02	3.04	0.83	0.01
Sat541	1.42	125.62	31.01	75.77	1.10	5.31	0.09	0.05	12.88	0.10	34.00	0.39	0.02	0.60	0.02	0.20	0.00	0.08	0.65	0.00

(continued on next page)

Table 1 (*continued*)

Fig. 1-2

Sample	V	Cr	Mn	Ni	Cu	Zn	Ga	Ge	As	Rb	Sr	Zr	Nb	Mo	Ag	Cd	In	Sn	Sb	Cs
Sat542	2.17	30.26	46.51	18.60	0.27	25.04	0.01	0.06	14.65	0.12	61.59	0.87	0.09	0.20	0.01	0.79	0.00	0.32	1.33	0.01
Sat543	3.79	9.01	69.77	3.77	0.19	5.30	0.03	0.00	13.63	0.03	34.56	0.25	0.04	0.51	0.02	0.32	0.01	0.48	1.00	0.02
Sat544	1.66	9.07	31.01	7.53	0.14	5.44	0.07	0.00	13.73	0.23	23.81	0.35	0.05	0.53	0.04	0.33	0.00	0.47	1.28	0.04
Sat545	1.21	5.37	108.53	3.98	0.32	24.12	0.00	0.08	11.29	0.01	28.83	0.37	0.04	0.31	0.01	0.21	0.01	0.93	12.99	0.00
Sat546	1.40	8.26	170.54	5.20	1.18	17.19	0.02	0.01	15.93	0.07	18.31	0.28	0.04	0.57	0.02	0.66	0.02	6.47	1.36	0.01
Average shale	99.00	71.00	927.00	56.00	39.00	76.00	16.00		1.50	108.00	342.00	142.00	14.00	3.00	0.05	0.23	0.08	4.00		3.70
Guojiaba average	328.48	85.06	438.47	64.92	32.80	121.78	16.20	1.36	24.54	90.74	224.98	195.15	10.36	17.21	0.36	1.30	0.11	2.55	3.90	4.59
Dengying average	6.25	24.83	289.04	18.61	1.70	17.94	0.36	0.05	16.50	1.48	84.73	2.32	0.22	1.18	0.02	0.32	0.01	1.12	2.15	0.13
Lower Guojiaba average	541.72	95.68	400.82	93.34	43.32	162.63	17.04	1.41	32.30	101.27	155.94	175.77	10.26	28.91	0.49	2.16	0.12	2.53	5.09	5.57
Upper Guojiaba average	86.80	73.02	481.14	32.70	20.88	75.49	15.25	1.30	15.75	78.79	303.23	217.11	10.47	3.96	0.20	0.34	0.10	2.58	2.56	3.48
Enrichment factors (Guojiaba Fm.)	3.32	1.20	0.47	1.16	0.84	1.60	1.01		16.36	0.84	0.66	1.37	0.74	5.74	7.13	5.67	1.39	0.64		1.24
Enrichment factors (upper Guojiaba Fm.)	0.88	1.03	0.52	0.58	0.54	0.99	0.95		10.50	0.73	0.89	1.53	0.75	1.32	4.00	1.47	1.29	0.64		0.94
Enrichment factors (lower Guojiaba Fm.)	5.47	1.35	0.43	1.67	1.11	2.14	1.07		21.53	0.94	0.46	1.24	0.73	9.64	9.89	9.38	1.47	0.63		1.51
Enrichment factors (Dengying Fm.)	0.06	0.35	0.31	0.33	0.04	0.24	0.02		11.00	0.01	0.25	0.02	0.02	0.39	0.38	1.40	0.12	0.28		0.04
Non-hydrothermal sediments		38.00		14.80		259.00				82.00	488.00	25.00		7.90						
Hydrothermal sediments		69.10		23.90		2044.50				100.00	454.00	51.90		12.30						

Fig. 1-3

Sample	Ba	Hf	Pb	Bi	Th	U	∑REE	∑LREE/∑HREE	Ce/Ce*	Eu/Eu*	Pr/Pr*	Y/Y*	$\delta^{13}C_{org}$ (‰)	TOC (%)	CRS (%)	$\delta^{34}S_{CRS}$ (‰)	V/Sc	V/Cr	V/(V+Ni)	Th/U
Sat531	532.67	4.20	8.05	0.07	7.69	2.32	157.42	3.23	0.94	1.17	1.01	0.99	−35.8	0.23	0.25	20.7	6.29	1.15	0.74	3.31
Sat530	1077.95	5.99	12.24	0.10	10.20	3.52	170.17	3.26	0.95	0.94	0.99	1.01	−31.1		0.23	23.0	6.76	1.21	0.73	2.90
Sat529	1194.87	5.07	10.07	0.12	10.33	2.90	165.02	3.13	0.93	1.00	1.02	0.97	−30.4	0.56	0.13	22.7	6.75	1.16	0.74	3.56
Sat528	1063.12	4.73	12.56	0.11	9.89	3.19	168.07	3.54	0.93	1.02	1.01	0.97	−30.1	0.38	0.39	19.2	7.32	1.16	0.70	3.10
Sat527	1208.01	6.68	10.86	0.11	10.80	3.01	170.17	3.06	0.93	0.97	1.01	0.96	−31.3		0.24	15.6	6.71	1.19	0.74	3.59
Sat526	1007.16	6.87	9.53	0.13	10.97	3.26	192.81	3.12	0.93	0.95	1.02	0.96	−30.9				5.69	1.13	0.74	3.37
Sat525	1358.89	6.79	10.76	0.14	10.61	3.81	171.76	3.29	0.92	1.00	1.02	0.95	−31.1	0.65	0.43	17.0	7.23	1.18	0.75	2.79
Sat524	1399.53	6.80	12.50	0.14	11.43	3.77	183.37	3.22	0.94	0.96	1.00	0.97	−30.5	0.69	1.20	19.2	7.01	1.24	0.70	3.03
Sat523	997.22	6.00	12.83	0.08	9.14	4.09	163.96	3.16	0.93	0.97	1.02	0.97	−31.5	0.81	0.44	17.1	7.11	1.14	0.71	2.24
Sat522	1314.47	7.47	12.73	0.16	11.89	4.57	206.67	3.67	0.92	0.92	1.04	0.93	−31.4	0.62	0.51	16.8	7.26	1.20	0.71	2.60
Sat521	1632.46	7.92	17.16	0.12	11.95	4.53	202.39	3.20	0.93	0.91	1.03	0.93	−31.3	0.87	0.39	16.5	7.21	1.25	0.72	2.64
Sat520	925.22	5.82	11.65	0.11	10.92	4.03	185.83	3.31	0.94	0.97	1.00	0.93	−31.4	0.77	0.41	18.2	7.43	1.23	0.72	2.71
Sat519	979.62	6.60	13.53	0.14	11.42	5.69	188.40	3.30	0.94	0.95	0.98	0.98	−31.2	1.13	1.31	15.1	6.67	1.13	0.74	2.01
Sat518	848.45	6.66	12.68	0.12	11.08	6.41	185.37	3.27	0.93	1.08	1.00	0.97	−31.7	1.32	0.69	15.6	7.12	1.20	0.74	1.73
Sat517	818.01	6.09	12.23	0.22	11.36	6.42	198.64	3.46	0.93	1.01	1.02	0.93	−32.1	1.63	0.81	12.3	7.48	1.23	0.74	1.77
Sat516	979.33	6.46	22.41	0.24	11.55	10.92	196.42	3.21	0.91	1.03	1.02	1.00	−33.9	1.74	1.27	−9.5	10.63	1.69	0.68	1.06

Sat515	1209.37	7.83	27.85	0.39	13.76	21.32	228.84	3.28	0.91	1.06	1.01	1.02	−34.2	1.88	1.43	−16.2	31.46	4.23	0.79	0.65
Sat514	10,436.27	2.91	15.88	0.08	3.54	13.29	157.88	1.28	0.88	1.36	0.98	1.15	−33.7				25.43	8.49	0.80	0.27
Sat513	1033.62	5.92	27.29	0.34	11.50	19.48	213.91	3.61	0.90	0.94	1.04	0.97	−34.6	3.17	0.22	−6.8	26.27	4.64	0.78	0.59
Sat512	993.12	5.82	26.11	0.30	11.32	18.41	208.65	3.58	0.91	0.92	0.96	0.84	−34.0	3.88	0.63	−1.4	26.56	4.40	0.78	0.61
Sat511	862.16	4.56	24.39	0.41	9.63	20.36	162.99	2.98	0.90	0.99	1.04	1.05	−33.8	3.15	1.30	1.0	23.21	3.45	0.72	0.47
Sat510	875.27	4.60	29.74	0.25	9.65	44.64	173.84	2.79	0.90	0.96	1.02	1.01	−34.0	4.08	0.91	3.6	14.44	2.17	0.73	0.22
Sat509	905.42	4.96	25.35	0.25	9.79	22.82	156.13	2.73	0.90	1.02	1.02	1.05	−34.2	3.11	1.60	3.7	95.58	11.48	0.88	0.43
Sat508	1005.75	4.76	23.49	0.32	10.12	17.30	185.75	3.05	0.88	1.00	1.01	1.07	−34.3	3.37	0.68	5.7	161.04	16.75	0.94	0.59
Sat507	930.50	5.46	22.05	0.28	10.42	16.11	183.30	2.91	0.88	1.02	1.02	1.07	−34.3	3.69	1.51	8.4	153.00	12.48	0.94	0.65
Sat506	965.18	6.58	37.57	0.24	11.84	23.40	190.26	3.00	0.90	0.88	1.01	1.04	−34.1	4.90	0.75	0.5	30.72	4.40	0.78	0.51
Sat505	1028.03	5.03	31.18	0.41	11.01	29.93	172.56	2.90	0.89	1.13	1.05	1.04	−34.5	4.18	0.94	−6.1	28.21	4.10	0.80	0.37
Sat504	1183.20	4.82	19.34	0.14	11.49	12.28	164.38	2.97	0.89	1.07	1.02	1.02	−34.8	3.12	1.30	7.7	13.27	2.09	0.74	0.94
Sat503	1140.71	5.11	12.93	0.15	11.77	8.71	195.25	3.47	0.88	0.94	1.06	0.98	−35.1	2.57	0.97	4.7	11.41	1.73	0.78	1.35
Sat502	1072.19	5.42	13.13	0.23	12.26	8.09	211.16	2.94	0.90	0.99	1.00	0.97	−34.8	0.85	0.50	7.5	8.88	1.58	0.75	1.52
Sat501	1516.90	5.62	21.22	0.28	12.45	5.62	146.17	5.47	0.91	1.13	1.00	1.03	−35.0				9.10	1.44	0.80	2.21
Sat500	116.51	0.39	11.33	0.05	1.06	9.28	60.88	1.57	0.68	1.02	1.01	1.52	−34.0				11.16	3.26	0.77	0.11
Sat533	38.02	0.04	0.72	0.01	0.07	0.39	4.13	1.05	0.68	0.60	0.93	1.93	−34.8	0.67			2.51	2.68	0.40	0.17
Sat534	32.09	0.01	0.81	0.00	0.03	0.56	5.97	0.79	0.62	1.12	0.90	1.87	−35.3	3.41			4.51	2.36	0.48	0.05
Sat535	120.60	0.37	5.07	0.03	1.17	1.28	25.95	3.16	0.85	0.93	1.07	1.19	−35.5				5.54	2.10	0.59	0.91
Sat536	62.82	0.13	9.42	0.02	0.46	0.45	12.67	3.62	0.97	1.48	0.89	1.48	−34.1	0.01			1.81	1.46	0.44	1.03
Sat537	38.08	0.17	3.34	0.01	0.50	2.08	12.55	2.67	0.75	0.83	1.04	1.59		0.50			2.66	1.92	0.54	0.24
Sat538	36.97	0.14	15.67	0.02	0.45	1.00	9.00	1.90	0.78	1.39	1.01	1.39	−35.6				1.83	1.34	0.47	0.44
Sat539	8.06	0.08	0.27	0.04	0.06	0.56	3.92	1.35	0.64	1.72	1.14	0.84		0.47			0.44	0.02	0.03	0.11
Sat540	7.45	0.00	0.97	0.01	0.03	0.84	0.92	5.14	0.97	4.08	0.86	0.90		0.39			0.72	0.11	0.15	0.04
Sat541	8.80	0.01	1.22	0.00	0.01	0.40								0.52			0.33	0.01	0.02	0.03
Sat542	6.30	0.03	15.90	0.01	0.11	1.06								0.30			0.49	0.07	0.10	0.11
Sat543	6.75	0.01	5.51	0.01	0.03	0.75								0.30			0.95	0.42	0.50	0.03
Sat544	9.44		8.25	0.01	0.04	0.57	0.64	3.58	1.05	3.36	0.76	1.78		0.35			0.43	0.18	0.18	0.07
Sat545	9.86	0.01	9.02	0.00	0.02	0.26	1.01	3.00	1.06	1.94	0.69	0.90		0.38			0.30	0.23	0.23	0.09
Sat546	10.79	0.01	12.84	0.02	0.02	0.35								0.00			0.36	0.17	0.21	0.05
Average shale	469.00	2.50	18.00		9.20	3.00														
Guojiaba average	1331.60	5.62	17.83	0.19	10.40	11.36														
Dengying average	28.29	0.08	6.36	0.01	0.21	0.75														
Lower Guojiaba average	1544.32	5.07	23.01	0.26	10.19	17.76														
Upper Guojiaba average	1090.51	6.24	11.96	0.12	10.64	4.10														
Enrichment factors (Guojiaba Fm.)	2.84	2.25	0.99		1.13	3.79														
Enrichment factors (upper Guojiaba Fm.)	2.33	2.50	0.66		1.16	1.37														
Enrichment factors (lower Guojiaba Fm.)	3.29	2.03	1.28		1.11	5.92														
Enrichment factors (Dengying Fm.)	0.06	0.03	0.35		0.02	0.25														
Non-hydrothermal sediments	148.60																			
Hydrothermal sediments	1079.30					14.02														

Table 2
REE (ppm) and trace element concentrations in the acid-insoluble fractions of sedimentary rocks from the Songtao section, Guizhou Province, South China

Fig. 2-1

Sample	Unit	Lithology	Depth (m)	La	Ce	Pr	Nd	Sm	Eu	Gd	Tb	Dy	Ho	Er	Tm	Yb	Lu	Y	Sc	Ti
Son594	Jiumenchong Fm.	Black shale	58.45	39.69	67.97	7.46	26.56	3.74	1.59	3.69	0.57	3.63	0.82	2.58	0.37	2.43	0.35	30.22	9.83	3916.17
Son593	Jiumenchong Fm.	Black shale	57.45	38.79	62.81	7.86	31.37	5.17	1.57	4.95	0.72	4.93	1.07	3.30	0.50	2.99	0.49	40.02	12.45	3550.90
Son592	Jiumenchong Fm.	Black shale	55.85	41.09	62.85	8.30	33.76	5.75	1.72	6.70	1.03	6.65	1.63	4.75	0.67	4.05	0.62	62.14	12.09	3736.53
Son591	Jiumenchong Fm.	Black shale	54.35	34.33	57.93	7.16	29.80	5.17	1.56	5.90	0.86	5.12	1.13	3.22	0.46	2.83	0.42	39.56	12.44	3197.60
Son590	Jiumenchong Fm.	Carbonate	51.45	10.89	18.46	2.62	11.13	2.32	1.06	2.74	0.39	2.60	0.54	1.84	0.22	1.42	0.22	24.72	5.77	1041.92
Son589	Jiumenchong Fm.	Black shale	50.3	28.19	48.31	6.45	25.16	5.25	1.46	5.60	0.78	4.83	1.11	3.10	0.46	2.96	0.43	36.83	11.72	2934.13
Son588	Jiumenchong Fm.	Black shale	49.6	36.63	55.22	7.43	29.66	5.79	1.68	6.53	0.98	5.94	1.28	3.70	0.53	3.34	0.49	47.99	11.46	2886.23
Son587	Jiumenchong Fm.	Black shale	48.6	34.32	48.24	7.17	30.30	5.40	1.40	6.15	0.91	5.65	1.30	3.92	0.56	3.59	0.53	46.48	10.02	2640.72
Son586	Jiumenchong Fm.	Black shale	47.95	7.71	8.54	1.08	4.35	0.81	0.80	1.16	0.16	1.28	0.34	1.16	0.17	1.07	0.18	21.22	3.04	191.62
Son585	Jiumenchong Fm.	Black shale	47.75	28.17	42.42	5.59	23.17	4.30	1.32	4.70	0.74	4.59	1.08	3.23	0.47	3.07	0.48	40.10	8.84	2137.72
Son584	Jiumenchong Fm.	Black shale	46	33.02	47.75	7.46	29.99	6.24	1.40	6.43	0.95	6.26	1.39	4.46	0.60	3.86	0.56	49.49	11.16	3017.96
Son583	Jiumenchong Fm.	Black shale	45	37.95	51.27	8.38	36.50	7.05	1.98	8.52	1.25	7.99	1.83	5.25	0.75	4.71	0.66	70.21	10.35	2928.14
Son582	Jiumenchong Fm.	Black shale	44.35	5.28	7.30	2.53	14.50	4.56	1.33	6.31	0.86	4.99	1.10	2.76	0.40	2.31	0.35	48.83	2.22	119.76
Son581	Jiumenchong Fm.	Black shale	44.15	42.50	40.30	8.96	41.85	8.94	1.88	11.16	1.66	11.43	2.87	9.04	1.36	7.75	1.17	114.34	9.88	2257.49
Son500	Liuchapo Fm.	Chert	44.05	1.45	1.77	0.43	1.97	0.64	0.11	0.76	0.13	1.04	0.20	0.75	0.12	0.54	0.10	8.63	0.93	83.83
Son501	Liuchapo Fm.	Chert	43.87	133.95	248.81	38.02	156.14	33.25	2.62	28.31	3.73	19.34	3.63	10.08	1.36	7.64	1.00	101.91	4.31	982.04
Son502	Liuchapo Fm.	Chert	43.52	1.88	1.83	0.47	2.23	0.58	0.15	0.71	0.10	0.67	0.17	0.56	0.08	0.52	0.07	7.21	0.87	53.89
Son503	Liuchapo Fm.	Chert	42.97	2.03	2.73	0.67	3.34	0.80	0.29	1.14	0.14	0.98	0.22	0.63	0.10	0.57	0.10	6.41	1.25	71.86
Son505	Liuchapo Fm.	Chert	38	1.17	1.32	0.33	1.43	0.39	0.11	0.47	0.09	0.44	0.11	0.35	0.05	0.37	0.07	3.47	1.20	47.90
Son506	Liuchapo Fm.	Chert	32	2.72	3.78	0.83	4.12	1.05	0.29	1.37	0.21	1.61	0.36	1.17	0.17	1.11	0.17	11.29	1.38	101.80
Son507	Liuchapo Fm.	Chert	28	5.00	6.88	1.18	4.85	0.88	0.20	0.99	0.17	1.10	0.23	0.77	0.09	0.73	0.12	7.22	1.96	419.16
Son508	Liuchapo Fm.	Chert	26	4.21	5.17	0.77	2.97	0.60	0.10	0.48	0.06	0.36	0.06	0.21	0.03	0.15	0.03	2.31	1.81	71.86
Son510	Doushantuo Fm.	Chert	23.6	13.94	26.78	2.80	10.04	1.83	0.42	1.87	0.31	1.66	1.08	1.11	0.16	1.08	0.14	10.84	4.65	1095.81
Son511	Doushantuo Fm.	Cherty shale	22.5	10.95	23.30	2.33	8.69	1.18	0.29	1.27	0.18	1.21	0.25	0.77	0.11	0.80	0.11	7.47	3.33	826.35
Son512	Doushantuo Fm.	Black shale	21.5	16.63	33.95	3.57	13.01	2.16	0.38	1.88	0.27	1.64	0.33	0.98	0.16	0.97	0.14	9.17	5.54	1526.95
Son513	Doushantuo Fm.	Black shale	20.5	11.25	18.36	2.13	7.85	1.62	0.31	1.47	0.19	1.10	0.25	0.80	0.10	0.65	0.07	6.97	4.15	724.55
Son514	Doushantuo Fm.	Black shale	19.5	38.51	62.51	7.71	28.16	4.82	0.83	5.15	0.73	4.82	1.13	4.00	0.62	4.18	0.66	34.91	11.86	3281.44
Son516	Doushantuo Fm.	Carboante	13.3	7.39	13.91	1.57	6.29	1.13	0.28	1.06	0.17	1.00	0.21	0.63	0.09	0.44	0.07	6.36	3.37	323.35
Son517	Doushantuo Fm.	Carboante	12.3	9.86	17.12	1.95	7.30	1.26	0.22	1.47	0.22	1.18	0.23	0.73	0.11	0.67	0.09	6.70	6.43	874.25
Son518	Doushantuo Fm.	Carboante	11.4	8.88	16.18	1.97	7.80	1.44	0.33	1.50	0.22	1.29	0.29	0.82	0.10	0.60	0.11	9.15	4.83	383.23
Son519	Doushantuo Fm.	Carboante	9.6	7.05	12.28	1.35	5.61	1.00	0.20	0.87	0.15	0.86	0.17	0.50	0.07	0.40	0.06	5.41	5.12	323.35
Son520	Doushantuo Fm.	Carboante	8.3	24.12	40.31	4.22	14.13	2.44	0.44	2.21	0.30	1.72	0.33	1.04	0.16	1.06	0.14	8.66	12.56	2712.57
Son521	Doushantuo Fm.	Carboante	7	8.81	17.28	2.07	8.20	1.35	0.35	1.55	0.21	1.25	0.25	0.74	0.09	0.55	0.09	7.53	5.63	329.34
	Nantuo Fm.	Tillite	0																	
Average shale	(Drever, 1988; Mclennan, 2001)																		10.00	
Doushantuo average																			6.13	1127.38
Liuchapo average																			1.71	229.04
Jiumenchong average																			9.38	2468.35
Enrichment factors (Doushantuo Fm.)																			0.61	
Enrichment factors (Liuchapo Fm.)																			0.17	
Enrichment factors (Jiumenchong Fm.)																			0.94	
Non-hydrothermal sediments	(Li and Gao, 1996)																			
Hydrothermal sediments																				

Fig. 2-2

Sample	V	Cr	Mn	Ni	Cu	Zn	Ga	Ge	As	Rb	Sr	Zr	Nb	Mo	Ag	Cd	In	Sn	Sb	Cs
Son594	475.48	83.83	15.50	45.68	11.32	13.63	14.69	1.31	25.95	78.33	119.85	156.83	11.04	111.94	1.06	0.26	0.03	2.45	16.00	2.92
Son593	2271.46	92.80	31.01	286.52	50.69	10.16	15.79	1.28	66.46	86.94	76.99	155.78	9.83	295.44	1.32	0.69	0.03	2.44	10.78	3.99
Son592	1418.17	99.51	38.76	328.77	79.95	48.78	16.53	1.03	59.94	79.77	106.12	185.04	10.17	216.61	1.28	1.37	0.03	2.14	13.32	3.56
Son591	563.96	74.33	116.28	141.80	51.88	94.50	16.30	0.82	51.07	71.19	88.99	147.92	8.71	90.22	1.35	1.32	0.05	1.96	5.05	2.90
Son590	581.48	42.96	1000.00	62.48	30.72	505.05	5.28	0.75	22.99	18.21	2829.68	45.13	2.73	17.97	1.09	12.33	0.03	1.09	3.40	0.80
Son589	685.75	70.84	201.55	168.54	69.64	246.94	12.88	0.90	64.50	72.73	75.47	131.77	8.53	112.44	4.77	2.37	0.02	1.55	15.65	3.27
Son588	1193.56	140.29	240.31	356.37	107.30	255.48	15.35	1.09	101.25	70.84	153.46	142.00	8.76	247.96	8.04	2.94	0.03	2.12	30.45	3.48
Son587	2001.25	109.02	46.51	384.41	68.81	180.93	13.89	0.98	77.12	70.47	181.22	135.43	8.04	143.61	5.43	4.82	0.02	1.06	20.41	3.59
Son586	200.77	7.41	674.42	33.05	12.80	23.72	1.70	0.30	17.67	1.34	2754.83	10.62	0.60	20.30	1.03	0.37	0.01	0.18	3.26	0.08
Son585	394.45	59.20	93.02	172.66	74.90	108.71	13.19	0.82	60.70	50.88	166.28	103.97	7.13	112.13	8.44	2.01	0.03	1.25	27.79	1.77
Son584	5602.03	440.59	69.77	273.90	324.99	4501.44	15.97	3.15	129.42	92.20	76.44	135.57	9.25	74.99	17.63	83.10	0.08	3.30	34.30	5.88
Son583	3850.46	174.70	449.61	321.49	105.19	1382.91	13.88	1.40	91.34	79.87	141.78	135.69	8.67	132.73	10.58	18.78	0.04	1.40	24.00	4.67
Son582	229.59	48.62	7.75	33.38	51.27	177.07	0.62	0.51	16.02	2.54	377.11	9.40	0.47	5.03	4.73	10.34	0.00	0.18	2.45	0.23
Son581	3246.95	1876.71	15.50	231.14	444.47	231.50	14.14	1.69	188.13	79.09	390.48	102.39	11.71	36.72	20.97	7.63	0.05	1.29	20.43	5.97
Son500	577.94	76.81	7.75	31.88	53.75	633.29	0.75	0.81	23.65	3.11	28.40	22.82	5.81	13.41	2.56	15.42	0.00	0.11	4.77	0.34
Son501	1394.04	9.12	147.29	31.82	57.24	450.26	42.51	2.48	190.80	113.60	381.96	243.68	37.82	34.65	4.39	16.28	0.05	2.51	19.09	10.25
Son502	274.89	60.42	7.75	28.29	47.71	175.54	0.47	0.51	19.08	2.19	36.37	7.16	0.32	11.28	2.05	2.35	0.01	0.03	4.14	0.27
Son503	110.63	50.07	7.75	32.32	63.26	76.73	0.71	0.44	16.23	2.65	32.53	13.87	0.48	9.78	0.23	1.01	0.01	0.63	1.69	0.28
Son505	163.39	47.82	7.75	15.55	22.23	11.80	0.39	0.24	15.65	1.76	36.74	13.59	0.50	3.25	0.10	0.32	0.00	0.14	0.91	0.20
Son506	247.97	74.25	15.50	26.37	49.90	13.42	0.99	0.29	16.92	4.23	46.18	41.68	0.77	3.10	0.36	0.46	0.01	0.74	1.46	0.38
Son507	43.55	25.42	7.75	5.45	5.62	7.09	2.68	0.42	16.03	14.52	18.36	19.91	1.19	0.68	0.15	0.11	0.00	0.55	0.83	0.78
Son508	7.48	4.16	3232.56	16.21	8.42	2.41	0.74	0.09	18.14	1.32	229.29	3.90	0.29	1.68	0.01	0.09	0.00	0.37	1.20	0.06
Son510	238.91	36.50	23.26	24.46	18.61	27.08	6.61	0.45	29.13	44.41	12.37	49.09	4.03	26.01	0.67	0.28	0.03	1.09	3.25	2.32
Son511	97.97	24.09	15.50	9.74	18.72	15.71	5.11	0.38	28.06	29.89	13.22	35.80	3.20	29.39	0.49	0.15	0.02	1.06	1.99	1.37
Son512	130.63	43.33	31.01	23.27	18.62	13.81	7.88	0.25	39.71	55.17	20.15	55.12	5.90	37.78	0.51	0.16	0.04	1.26	3.80	2.71
Son513	223.50	22.96	1279.07	12.25	5.51	28.50	4.15	0.40	21.81	26.02	119.54	23.98	2.50	7.53	0.19	0.17	0.02	0.76	1.04	1.65
Son514	1085.02	178.24	23.26	34.46	57.41	79.50	17.50	1.01	45.16	128.72	26.47	115.25	10.97	45.31	12.86	1.44	0.07	3.99	14.64	7.72
Son516	33.44	19.47	426.36	21.36	3.59	8.09	1.82	5.41	12.62	12.53	175.01	10.63	1.15	0.44	0.06	0.56	0.01	0.39	0.85	0.72
Son517	93.82	38.81	666.67	11.57	4.60	34.80	5.00	0.28	13.41	36.59	135.14	29.65	2.99	0.56	0.01	0.99	0.03	1.15	0.79	1.96
Son518	59.57	21.63	286.82	13.49	5.11	15.29	2.32	0.11	14.41	14.15	179.14	13.94	1.37	0.11	0.00	1.16	0.01	0.50	0.64	0.75
Son519	90.36	29.10	248.06	15.98	2.75	8.95	1.84	0.14	13.25	12.49	168.87	10.22	1.08	0.19	0.02	0.75	0.02	3.50	1.14	0.63
Son520	364.73	91.10	341.09	31.57	33.05	129.47	15.56	1.20	16.17	108.23	99.99	84.30	9.25	0.49	0.12	2.71	0.07	3.74	2.45	6.41
Son521	60.40	17.98	232.56	15.19	2.88	10.85	1.98	0.10	12.64	12.96	202.85	10.70	1.22	0.26	0.03	0.84	0.01	0.84	1.36	0.61
Average shale	99.00	71.00	927.00	56.00	39.00	76.00	16.00		1.50	108.00	342.00	142.00	14.00	3.00	0.05	0.23	0.08	4.00		3.70
Doushantuo average	225.30	47.56	324.88	19.39	15.53	33.82	6.34	0.88	22.40	43.74	104.80	39.88	3.97	13.46	1.36	0.84	0.03	1.66	2.90	2.44
Liuchapo average	352.49	43.51	429.26	23.49	38.52	171.32	6.15	0.66	39.56	17.92	101.23	45.83	5.90	9.73	1.23	4.50	0.01	0.63	4.26	1.57
Jiumenchong average	1622.52	237.20	214.29	202.87	106.00	555.77	12.16	1.14	69.47	61.03	538.48	114.11	7.54	115.58	6.27	10.59	0.03	1.60	16.23	3.08
Enrichment factors (Doushantuo Fm.)	2.28	0.67	0.35	0.35	0.40	0.45	0.40		14.93	0.41	0.31	0.28	0.28	4.49	27.15	3.64	0.36	0.42		0.66
Enrichment factors (Liuchapo Fm.)	3.56	0.61	0.46	0.42	0.99	2.25	0.38		26.38	0.17	0.30	0.32	0.42	3.24	24.62	19.59	0.15	0.16		0.42
Enrichment factors (Jiumenchong Fm.)	16.39	3.34	0.23	3.62	2.72	7.31	0.76		46.31	0.57	1.57	0.80	0.54	38.53	125.32	46.06	0.39	0.40		0.83
Non-hydrothermal sediments		38.00		14.80		259.00				82.00	488.00	25.00		7.90						
Hydrothermal sediments		69.10		23.90		2044.50				100.00	454.00	51.90		12.30						

(continued on next page)

Table 2 (*continued*)

Fig. 2-3																				
Sample	Ba	Hf	Pb	Bi	Th	U	∑REE (ppm)	∑LREE/ ∑HREE	Ce/ Ce*	Eu/ Eu*	Pr/Pr*	Y/Y*	$\delta^{13}C_{org}$ (‰, PDB)	TOC (%)	$\delta^{34}S_{CRS}$ (‰,CDT)	TS (%)	V/Sc	V/Cr	V/(V+ Ni)	Th/U
Son594	22923.71	4.85	49.00	0.31	11.18	39.40	191.68	3.29	0.91	2.01	1.03	1.40	−33.0		12.2	1.12	48.4	5.67	0.91	0.28
Son593	11720.33	4.41	45.35	0.33	10.28	44.61	206.53	2.50	0.83	1.46	1.04	1.39	−33.1		9.4	3.03	182.4	24.48	0.89	0.23
Son592	15857.36	5.57	54.20	0.37	9.80	76.53	241.67	1.74	0.78	1.29	1.05	1.50	−32.9		5.2	3.67	117.3	14.25	0.81	0.13
Son591	14136.05	4.51	31.05	0.27	8.80	48.09	195.43	2.29	0.85	1.32	1.01	1.31	−33.0		2.5	3.98	45.3	7.59	0.80	0.18
Son590	3912.43	1.30	9.30	0.09	2.82	10.66	81.16	1.34	0.80	1.95	1.06	1.67	−33.7		8.2	1.11	100.8	13.54	0.90	0.26
Son589	11363.24	3.84	47.05	0.25	8.00	59.60	170.90	2.05	0.83	1.25	1.08	1.27	−33.4		0.2	3.93	58.5	9.68	0.80	0.13
Son588	9023.31	3.87	73.25	0.32	8.49	98.47	207.18	1.93	0.77	1.27	1.07	1.39	−33.4		−5.0	4.86	104.1	8.51	0.77	0.09
Son587	5964.80	3.72	40.80	0.25	7.69	45.89	195.93	1.84	0.71	1.13	1.08	1.37	−33.2		2.4	3.70	199.8	18.36	0.84	0.17
Son586	4403.85	0.32	8.84	0.03	0.57	16.84	50.05	0.87	0.66	3.74	1.04	2.57	−32.4		6.3	0.38	66.0	27.10	0.86	0.03
Son585	8868.35	2.99	46.76	0.23	6.97	65.73	163.42	1.80	0.78	1.37	1.04	1.44	−33.1		3.5	4.00	44.6	6.66	0.70	0.11
Son584	7619.33	3.87	52.73	0.32	8.61	42.91	199.84	1.70	0.70	1.03	1.14	1.34	−33.9		7.4	2.88	502.0	12.71	0.95	0.20
Son583	7946.08	3.69	49.00	0.29	8.59	48.16	244.30	1.41	0.66	1.19	1.10	1.46	−34.2		5.1	3.36	371.9	22.04	0.92	0.18
Son582	1838.13	1.57	5.93	0.03	0.29	18.39	103.40	0.52	0.43	1.13	1.10	1.66	−34.1	1.94	3.3	0.62	103.4	4.72	0.87	0.02
Son581	7625.78	3.08	45.46	0.53	7.35	48.58	305.19	0.90	0.48	0.87	1.17	1.59	−33.6	3.25	9.0	3.20	328.6	1.73	0.93	0.15
Son500	1585.79	2.62	5.70	0.02	0.29	11.53	18.64	0.52	0.51	0.77	1.22	1.50	−34.2	0.80	9.2	0.11	624.8	7.52	0.95	0.03
Son501	45,492.81	14.96	61.11	0.82	31.10	51.79	789.77	3.46	0.80	0.40	1.11	0.97	−32.5	0.26	11.4	1.85	323.8	152.89	0.98	0.60
Son502	377.11	2.93	3.99	0.03	0.22	6.85	17.21	0.71	0.45	1.09	1.19	1.69	−33.7	2.32	11.2	0.10	317.4	4.55	0.91	0.03
Son503	735.51	3.26	2.01	0.02	0.41	7.61	20.13	0.96	0.53	1.40	1.14	1.11	−34.5	1.09	13.8	12.50	88.4	2.21	0.77	0.05
Son505	240.13	2.98	1.60	0.02	0.24	2.98	10.17	0.88	0.49	1.23	1.27	1.24	−34.5	1.25			136.5	3.42	0.91	0.08
Son506	187.21	3.68	2.34	0.03	0.59	4.89	30.24	0.73	0.58	1.11	1.11	1.18	−34.3	4.60			179.4	3.34	0.90	0.12
Son507	1120.54	4.73	1.91	0.04	1.14	1.99	30.40	1.66	0.65	1.02	1.17	1.14		0.60	1.5		22.2	1.71	0.89	0.57
Son508	60.07	0.25	2.84	0.02	0.35	0.73	17.50	3.75	0.66	0.90	1.14	1.21	−33.0	0.31			4.1	1.80	0.32	0.48
Son510	615.37	1.80	15.77	0.20	5.66	10.00	74.05	3.06	0.99	1.05	1.00	0.56	−31.7	5.48			51.4	6.55	0.91	0.57
Son511	522.85	1.50	13.64	0.14	4.22	9.55	58.89	3.84	1.06	1.10	0.96	1.09	−29.5	10.43			29.5	4.07	0.91	0.44
Son512	756.17	1.86	22.67	0.30	7.12	10.24	85.22	4.49	1.02	0.88	1.00	1.00		13.06			23.6	3.01	0.85	0.70
Son513	296.26	1.02	3.34	0.13	3.59	2.94	53.12	3.58	0.86	0.94	1.04	1.06	−34.6	2.71			53.9	9.73	0.95	1.22
Son514	1309.53	3.46	90.06	1.03	14.57	11.58	198.73	2.54	0.83	0.77	1.08	1.19	−34.8	4.54			91.5	6.09	0.97	1.26
Son516	140.89	0.45	4.37	0.05	1.53	5.33	40.59	3.05	0.94	1.21	0.99	1.11		1.21			9.9	1.72	0.61	0.29
Son517	423.00	0.92	4.23	0.20	4.16	2.20	49.10	3.31	0.90	0.76	1.03	1.02	−35.7	0.07			14.6	2.42	0.89	1.89
Son518	235.92	0.35	5.97	0.10	1.63	3.09	50.68	2.60	0.89	1.05	1.03	1.20		1.29			12.3	2.75	0.82	0.53
Son519	155.25	0.29	4.45	0.14	1.55	2.79	36.00	3.24	0.91	1.03	0.96	1.12		0.03			17.6	3.10	0.85	0.56
Son520	994.11	2.44	20.18	0.62	12.19	3.52	101.25	5.49	0.91	0.89	1.03	0.92		0.04	−23.4		29.0	4.00	0.92	3.47
Son521	155.12	0.30	3.47	0.08	1.49	1.95	50.28	3.11	0.93	1.12	1.02	1.09		0.00			10.7	3.36	0.80	0.76
Average shale	469.00	2.50	18.00		9.20	3.00														
Doushantuo average	509.50	1.31	17.10	0.27	5.25	5.74														
Liuchapo average	6224.90	4.43	10.19	0.12	4.29	11.05														
Jiumenchong average	9514.48	3.40	39.91	0.26	7.10	47.42														
Enrichment factors (Doushantuo Fm.)	1.09	0.52	0.95		0.57	1.91														
Enrichment factors (Liuchapo Fm.)	13.27	1.77	0.57		0.47	3.68														
Enrichment factors (Jiumenchong Fm.)	20.29	1.36	2.22		0.77	15.81														
Non-hydrothermal sediments	148.60																			
Hydrothermal sediments	1079.30					14.02														

4. Results

Analytical results are presented in Tables 1 and 2. Enrichment factors, which are calculated as mean elemental concentration/average shale (PAAS) or upper continental crust (UCC) according to Mclennan (2001), are shown in Fig. 5. Both sections exhibit similarities in trace element abundances with significant enrichments of Mo>Cd>V>U>Ni>Ag>Zn>Cu>Pb for black shales of the lower Guojiaba Formation relative to grey shale of the upper Guojiaba Formation (Shatan section) and As>Ag>Mo>Cd>V>U>Ba>Zn>Ni relative to UCC. Black shales of the Jiumenchong Formation (Songtao section) are enriched with As>Ag>Cd>Mo>Ba>V>U>Zn>Ni>Cr>Cu>Pb relative to UCC, while similar enrichments are found for two samples of chert, in particular, at the top of the Liuchapo Formation (Songtao section).

Songtao and Shatan section samples show a range of total REE concentrations from <1 ppm to 790 ppm. Neither black shale nor carbonate samples from the Shatan section (Fig. 6) exhibit significant deviations from flat REE patterns with $Ce/Ce^*_{avg.}=0.89\pm0.1$ ($n=42$). Normalized REE concentrations in samples of Shatan section black shales are thus typical for bulk shale (Fig. 6); however, REE distribution patterns of Songtao section samples, in particular, black shales and chert (Fig. 7), are anomalously depleted in Ce with $Ce/Ce^*_{avg.}=0.76\pm0.17$ ($n=33$). Black shales of the Jiumenchong Formation (Fig. 7) exhibit both positive Eu anomalies ($Eu/Eu^*_{avg.}=1.5\pm0.7$, $n=14$), positive Y anomalies and negative Ce anomalies ($Ce/Ce^*_{avg.}=0.73\pm0.14$, $n=14$), which contrast with the more featureless patterns of black shale samples from the Shatan section with $Eu/Eu^*_{avg.}=1.01\pm0.09$ ($n=32$) and $Ce/Ce^*_{avg.}=0.91\pm0.05$ ($n=32$).

5. Discussion

5.1. Trace element geochemistry

The origin of the Ni–Mo–V–U-enriched Lower Cambrian "black rock series" in South China has been researched for many years, but its genesis is still controversial and insufficiently understood. Several hypotheses based on geological investigations and analytical data have been put forward, such as: (1) extra-terrestrial sources

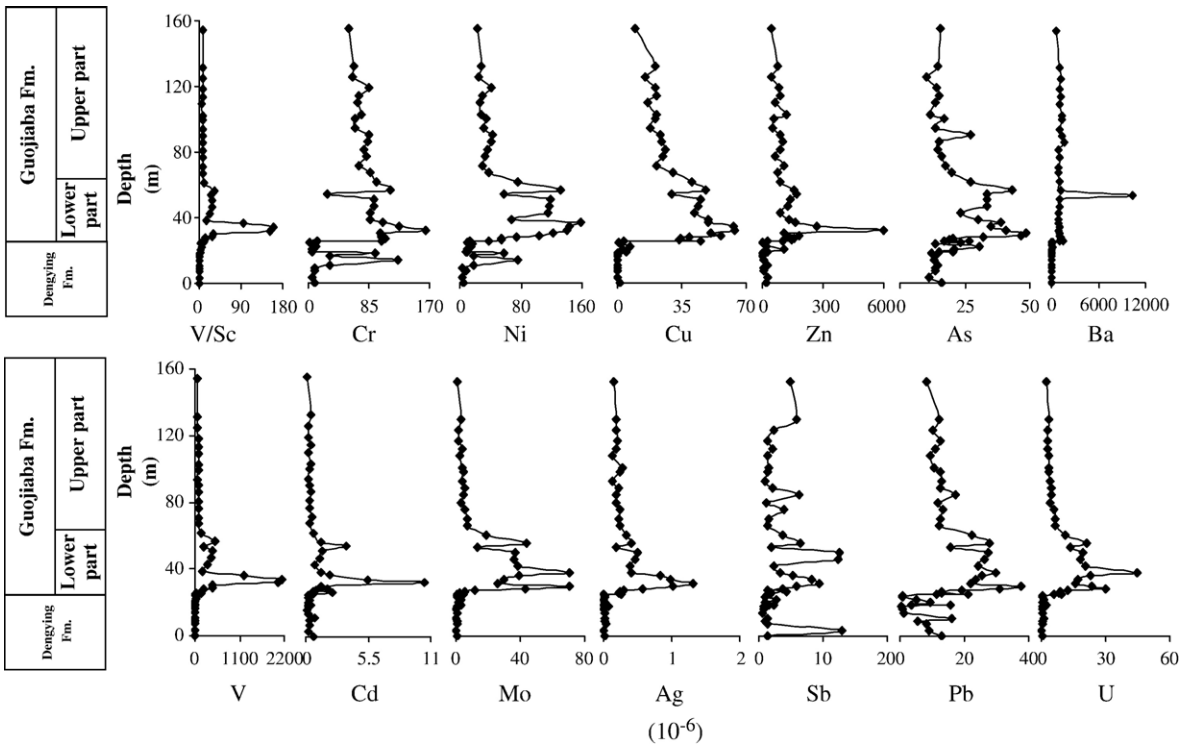

Fig. 3. Stratigraphic distribution of trace element concentrations (ppm) in Neoproterozoic–Lower Cambrian sedimentary rocks of the Shatan section, Sichuan Province, South China.

(Fan, 1984); (2) submarine hydrothermal exhalative origin (Steiner et al., 2001; Lott et al., 1999); (3) organosedimentary marine sedimentation (Mao et al., 2002).

5.1.1. Th/U ratios

The actinide metals uranium (U) and thorium (Th) exhibit similar geochemical characteristics, except under oxidizing conditions (Rogers and Adams, 1976; Wedepohl et al., 1978; Liu et al., 1984). Thorium is relatively unaffected by redox conditions and remains as insoluble Th^{4+} in the marine environment; however, soluble U^{6+} is favoured under oxidizing conditions. Under strongly reducing conditions within the sediment, U^{6+} (uranyl carbonate) may be reduced to the immobile U^{4+} fluoride complex, leading to U enrichment in sediments, while oxidizing conditions can lead to U loss from sediments overlain by oxidized bottom waters. Average shale, which integrates the composition of the upper continental crust, has a Th/U ratio of 3.8. Under normal oxidizing conditions, marine shales ought to retain this ratio or higher because the soluble form of U will be favoured; however, some U may be sequestered during early diagenesis because of reducing conditions in pore waters related to organic decomposition. Wignall and Twitchett (1996) have suggested that environments characterized by anoxic conditions lead to shale Th/U ratios of 0 to 2, and this general guideline has been followed in subsequent studies. Kimura and Watanabe (2001) showed, for example, that only samples with Th/U ratios below 2 exhibited no recognizable bioturbation in Early Cambrian shales of Iran, thus confirming that Th/U = 2 was an appropriate cut-off point between oxic and anoxic bottom-waters in that study (Table 3).

Black shales of the Guojiaba Formation (Shatan section) exhibit a wide range of Th/U ratios that rise stratigraphically in an oscillatory fashion from 0.22 to 3.6 (Fig. 8), which suggests that the depositional environment changed progressively from anoxic to oxic through time. An exception is found at the very base of the Lower Guojiaba Formation, the siliceous Kuanchuanpu Member, which exhibits higher Th/U ratios up to 2.2. Samples from the Songtao section also yielded low Th/U ratios below 2, except for one sample

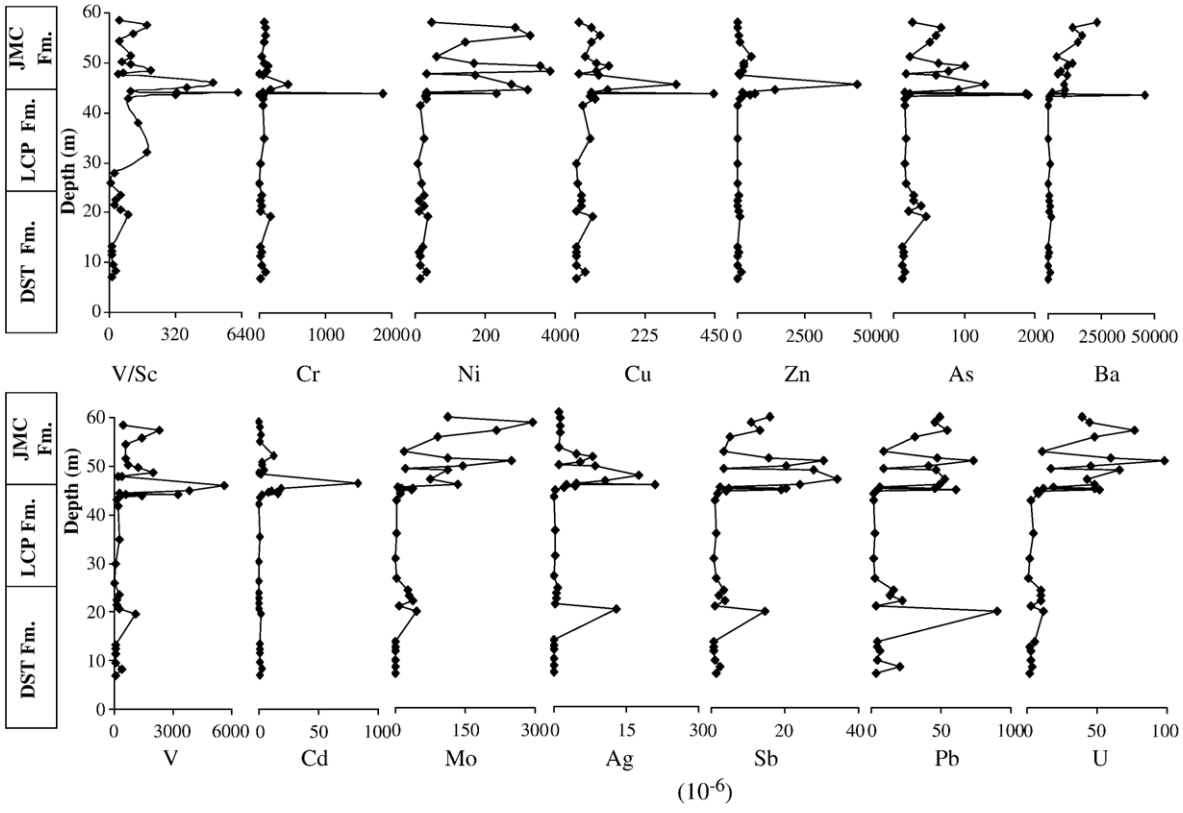

Fig. 4. Stratigraphic distribution of trace element concentrations (ppm) in Neoproterozoic–Lower Cambrian sedimentary rocks of the Songtao section, Guizhou Province, South China.

in the carbonate-rich Doushantuo Formation that has a Th/U ratio of 3.5 (Fig. 9; Table 2). Organic-rich black cherts of the Liuchapo Formation and black shales of the Jiumenchong Formation both contain samples with extreme Th/U ratios as low as 0.02, compared with a lowermost ratio of 0.22 from black shales of the Shatan section, which suggests that the Songtao section experienced a more reducing environment than the shallower Shatan section. By comparison with published Th/U studies (e.g. Kimura and Watanabe, 2001), redox conditions in bottom waters seem to have remained anoxic throughout the interval of metal enrichment in both parts of the basin.

5.1.2. Vanadium (V/Sc, V/Cr, V/(V+Ni) systematics

Vanadium is a redox-sensitive element that is preferentially enriched in sediments underlying anoxic or near-anoxic waters (Calvert and Pedersen, 1993). Kimura and Watanabe (2001) propose that the degree of enrichment is best expressed as the V/Sc ratio because the reduced form of V and Sc are equally insoluble, while V abundance in shales varies relative to Sc and not to other generally insoluble elements, such as Ti or Al. Those authors showed that significant V enrichment over Sc (up to 24 in their study) only occurred in samples that also exhibit Th/U ratios lower than 2, that is in samples that were most likely deposited beneath anoxic bottom waters. In our study, Guojiaba Formation samples exhibited V/Sc enrichments of the same magnitude to those reported by Kimura and Watanabe (2001) in samples with Th/U < 1.5 (the lowest Th/U ratio reported in that study) but considerably greater enrichments in samples with Th/U < 0.8 (Fig. 10D). Identical relationships were found for the Songtao section samples (Fig. 11H) in both chert and black shale, with V/Sc ratios as high as 600. Because of the extremely low Th/U ratios and high V/Sc ratios in our study relative to comparative studies where bottom waters were clearly anoxic, it seems to us highly plausible that bottom waters on the Yangtze Platform shelf were occasionally sulphidic (euxinic). It is not possible based on available data to ascertain whether euxinia reached into the photic zone. V/(V+Ni) values are high (>0.7) to extremely high (>0.9) throughout the shales of both sections Tables 1 and 2, which has been considered in other studies to indicate anoxic to euxinic bottom water conditions (Rimmer, 2004).

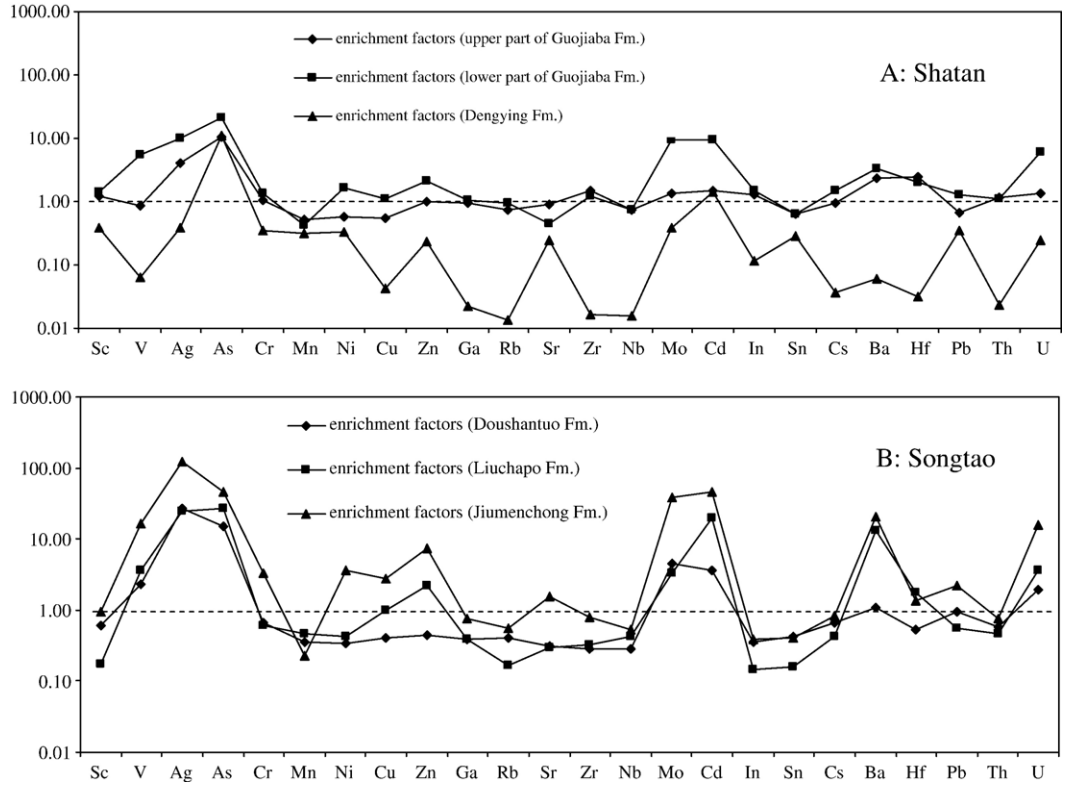

Fig. 5. Trace element enrichment factors relative to average shale or Upper Continental Crust (Mclennan, 2001) in sedimentary rocks of the Shatan (A) and Songtao (B) sections.

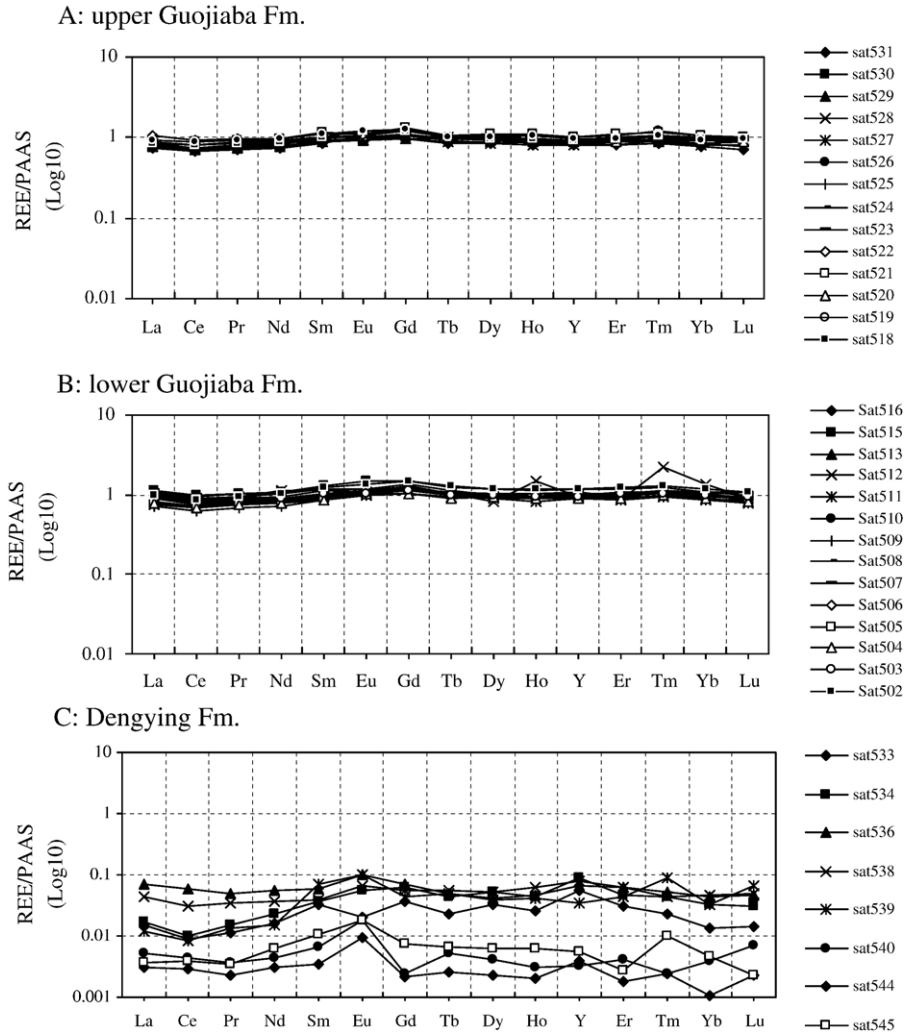

Fig. 6. Shale-normalized REE distribution spectra of Neoproterozoic–Lower Cambrian sedimentary rocks from the Shatan section, Sichuan Province, South China.

5.1.3. Rare earth element distributions and cerium anomalies

The conservative nature of the rare earth elements (REE) as a group and the anomalous behaviour of cerium (Ce) within this group could provide limited potential for distinguishing anoxic and oxic palaeoenvironments in the same way as Th/U and V/Sc ratios. Normal seawater contains anomalously low concentrations of Ce because it is the only rare earth element that can easily be oxidized to its relatively insoluble 4+ valence state under normal surface conditions. Marine authigenic precipitates (carbonates, phosphates, cherts) may retain this seawater Ce anomaly, in which case oxic bottom waters are indicated (Holser, 1997; Shields and Stille, 2001). It has been suggested that shales may retain an inverse form of this Ce anomaly, because Ce^{4+} would remain immobile under oxic conditions, would tend to be lost from sediments under more reducing conditions (Wilde et al., 1996). A comparable phenomenon leads to Mn enrichment in shales deposited under oxic conditions (Calvert and Pedersen, 1993).

Ce anomalies in Upper Guojiaba Formation grey shales (TOC < 1%) are remarkably consistent ranging from 0.94 to 0.96 and are significantly higher than Ce anomalies in the Lower Guojiaba Formation black shales, which range from 0.89 (0.69 in the basal Kuanchuanpu Member chert) to 0.93. Ce depletion is apparent in both parts of the Guojiaba Formation, but is more significant in the lower part, which we have concluded on the basis of Th/U ratios was deposited under more reducing conditions. These relative differences concur with the expectations of Wilde et al. (1996); however, because Wilde

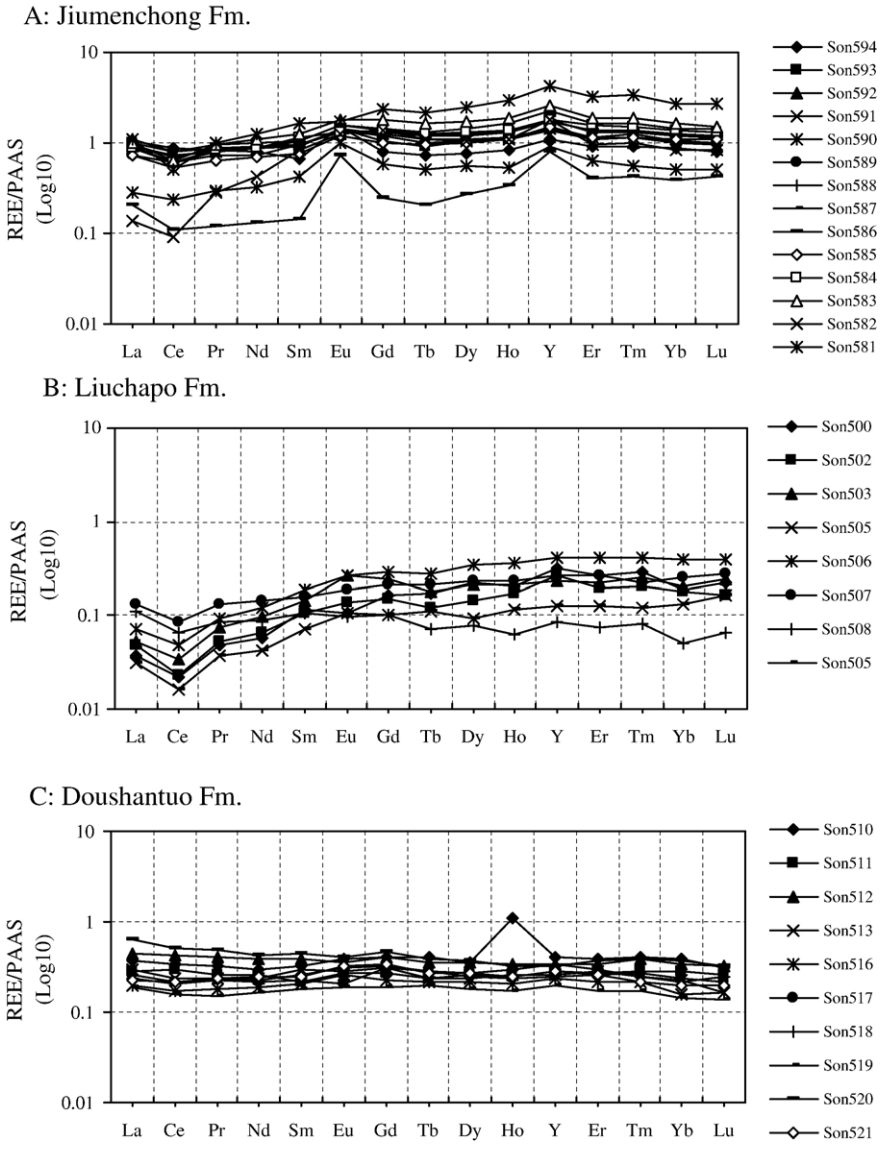

Fig. 7. Shale-normalized REE distribution spectra of Neoproterozoic–Lower Cambrian sedimentary rocks from the Songtao section, Guizhou Province, South China.

et al.'s predictions seem only to be valid for positive Ce anomalies in the acid-insoluble fractions of shales, it seems likely that the difference is due more to sediment source than to redox conditions. Pr/Pr∗ ratios average 1.01 and 1.02, in the upper and lower Guojiaba Formation, respectively, which indicates that these Ce anomaly

Table 3
Th and U concentrations and Th/U ratios in the acid-insoluble fractions of sedimentary rocks (Rogers and Adams, 1976; Wedepohl et al., 1978; Liu et al., 1984)

Fig. 3 Lithology	Sr (ppm)	Ba (ppm)	Th (ppm)	U	Th/U	Sr/Ba
Pure carbonate	610	10–30	0.05–2.4	0.03–2.2	0.02–1.1	60–20
Normal shale	300	10–546	10–13	3.7	2.7–7	0.5–5
Black shale	<300	546–5000	10–15	8.00	1.3–4	0.05–0.5

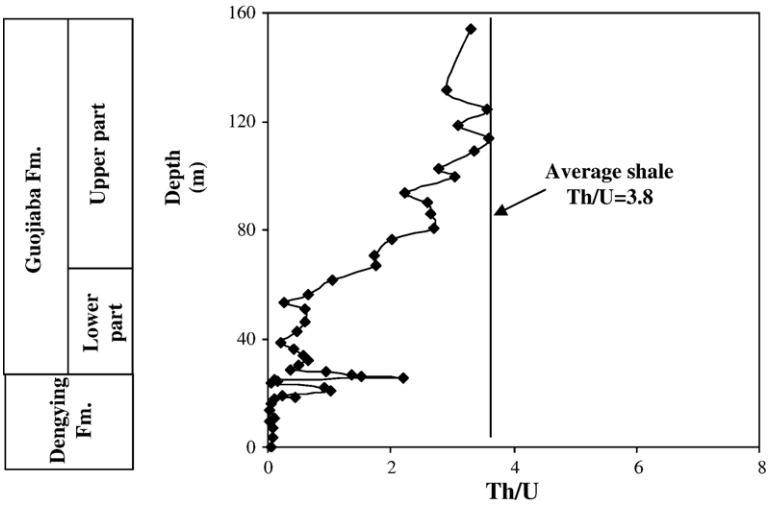

Fig. 8. Th/U ratios of Neoproterozoic–Lower Cambrian sedimentary rocks from the Shatan section, Sichuan Province, South China.

differences are very subtle indeed and may have been artificially enhanced by variable La concentrations (Bau and Dulski, 1996).

Negative Ce anomalies are also apparent in black shales of the Songtao section with significant departures from average shale (Fig. 7; Table 2). Generally high Pr/Pr* values (>1.1) confirm the genuine nature of these negative Ce anomalies in four samples of black shale and all samples of chert from the Liuchapo Formation, all of which exhibit seawater-like patterns of 1) HREE enrichment, 2) Y/Y* enrichment, 3) slight Gd enrichment, as well as very low Mn concentrations (Table 2). Several samples with extreme Ce depletion contained the lowest Th/U ratios of all the analysed samples (Th/U=0.02–0.03), thus contradicting all other measured redox proxies, which indicated that the sediments were deposited under extremely reducing conditions. This contradiction suggests that the chert, and presumably also silica within the black shale, formed within the water column above a redox boundary and not within the sediment. The most likely explanation seems to be that silica in both sections originated within the more oxic surface waters, possibly as biosiliceous tests (Braun et al., 2003) or as precipitated colloidal silica

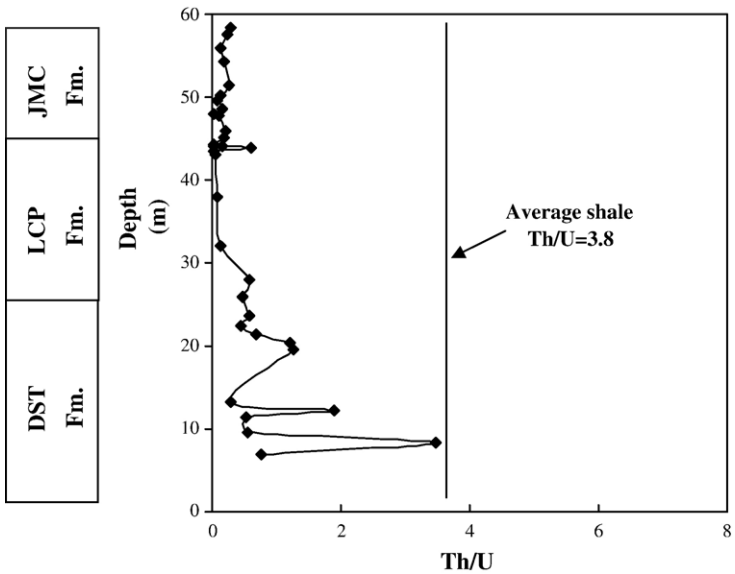

Fig. 9. Th/U ratios of Neoproterozoic–Lower Cambrian sedimentary rocks from the Songtao section, Guizhou Province, South China.

(Grenne and Slack, 2003), and these two possible interpretations are explored below.

5.1.4. Europium anomalies

Europium anomalies are negligible in the black shale samples of the Shatan section. However, positive Eu anomalies characterize some black shale samples of the Songtao section, for example, sample Son 586, which also shows no Ce depletion, but does exhibit seawater-like HREE enrichment and a positive Y anomaly. Europium is found enriched in highly reducing hydrothermal fluids (Michard and Albarède, 1986; Olivarez and Owen, 1991), and positive Eu anomalies are very common in marine hydrothermal sediments (Douville et al., 1999; Murray et al., 1991; Owen et al., 1999; Ruhlin et al., 1986). If the Eu anomaly derived from a hydrothermal source, then this hydrothermal signature must have been strongly modified by seawater because of the characteristic carbonate complexation signature of HREE depletion and Y enrichment in the samples. It seems likely, therefore, that any hydrothermal imprint was imparted to the chert sample within the water column (cf. Grenne and Slack, 2003).

5.2. Metal enrichment in the Niutitang Formation

It has been reported widely that Mo concentrations parallel TOC in black shales, e.g. Wilde et al. (2004), and this study is no exception. Mo concentrations in the Shatan section (Figs. 3 and 12) show convincing correlation with TOC and to a lesser extent, Ni, Cu and U. Low Th/U ratios and high V concentrations imply anoxic, possibly euxinic conditions during metal sequestration, which are likely to have been caused by fermentative oxidation of this excess organic matter. This possibility is consistent with low $\delta^{13}C_{org}$ values, −35‰ to −34‰, which are enigmatically correlated with low $\delta^{34}S_{pyr}$ values down to −16‰, which is at least 50‰ lower than contemporaneous seawater (Shields et al., 1997). Cruse and Lyons (2004) report similarly elevated S-isotopic discriminations for Carboniferous black shales and interpret those sulphides as having formed in an open environment that was not sulphate limited, i.e. seawater. We concur with their interpretation and propose that sulphate-reduction occurred in seawater overlying black shales of the Guojiaba Formation, which implies that bottom waters were occasionally euxinic on the Yangtze Platform during the Early Cambrian.

The rare presence of elevated Mn concentrations in one sample from the Shatan section (Fig. 5) indicates that bottom waters were oxic during deposition of that sample (Calvert and Pedersen, 1993). The same sample also contains high Ba concentrations (>1%), an order of magnitude higher than any other sample (Fig. 3), which indicates the presence of the mineral barite and by implication a sulphate/sulphide redox front for that sample within the sediment rather than within the water column (Torres et al., 2003). A similar Ba spike is also apparent from the Songtao section (Fig. 4). These spikes

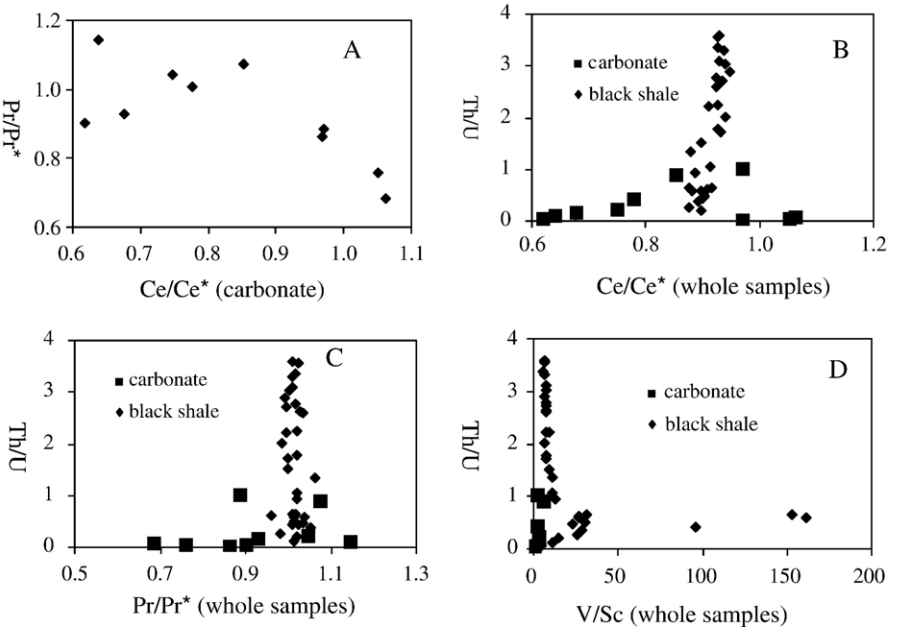

Fig. 10. Binary cross-correlation plots of various geochemical parameters for Shatan section samples.

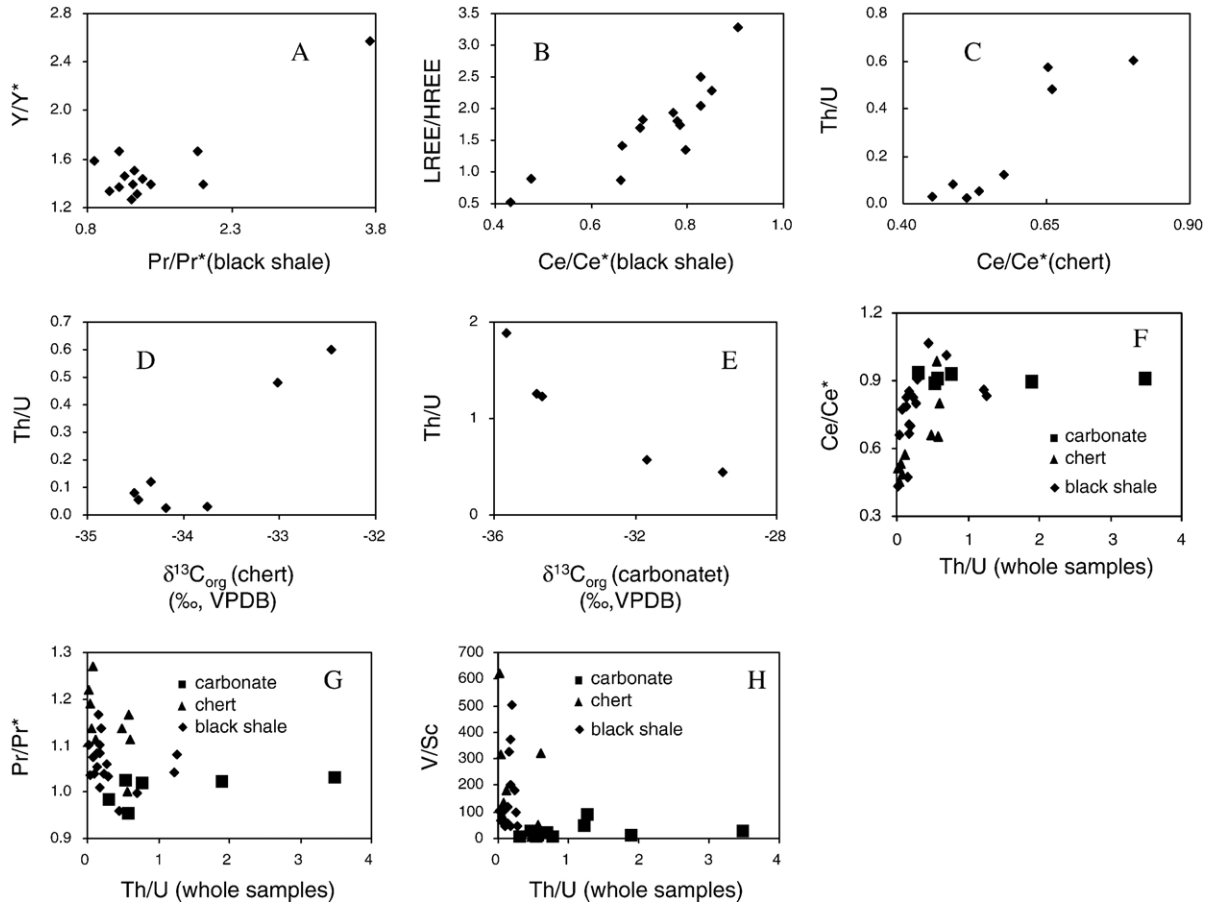

Fig. 11. Binary cross-correlation plots of various geochemical parameters for Songtao section samples.

mark rare, transient increases in the oxidation state of bottom waters that followed the build up of Ba in euxinic pore waters.

Europium anomalies are generally absent from metal-enriched samples of both sections, which suggests that hydrothermal activity did not play an active role in metal transport. Nevertheless, the hydrogenous REE signatures of cherts and black shales from the Songtao section do contain positive Eu anomalies, which suggests that basin seawater was indeed influenced by the expulsion of fluid plumes from spreading ridges. Hydrothermal plumes could have provided some of the redox-sensitive metals that became enriched in the black shales as well as the hydrogenous silica, the origin of which is discussed in more detail below.

5.3. Silicification

It was established above that the negative Ce anomalies and seawater-like REE patterns of the Songtao section samples, in particular, derived from precipitation of silica above a redox boundary in the water column. There is no indication that there was a direct hydrothermal influence over chert formation as it generally lacks a Eu anomaly and, apart from the very top of the Liuchapo Formation, is not particularly enriched in any metal. Organic matter in the chert beds show the same positive correlation with $\delta^{13}C_{org}$ (Fig. 11D) as at Shatan, suggesting perhaps that anoxic fermentation (oxidation) processes were responsible for the anoxic conditions; however, an equally convincing correlation is apparent between Th/U ratios and Ce depletion (Fig. 11C). These apparently contradictory results indicate that there was a genuine correlation between enhanced, reducing conditions (and organic matter recycling) and Ce depletion in the silica-rich fluids that replaced the organic-rich muds during early diagenesis. This would be consistent with a biogenic origin for the silica because both Th/U and Ce depletion could relate to organic productivity in the photic zone.

In this scenario, siliceous phytoplankton, such as radiolaria, retained the seawater REE signature of the oxygen-rich, photic zone, later imparting it to the sediment during diagenesis. The alternative hypothesis that silica precipitated abiotically or by microbial mediation from seawater due to the flocculation effects of iron oxyhydroxides from ridge plumes (Grenne and Slack, 2003) seems unlikely because of the retention of seawater-like Sm/Yb ratios and the absence of a positive Eu anomaly in these cherts. In addition, anoxic conditions in bottom waters would have greatly limited the formation and/or survival of iron oxyhydroxides from any source, hydrothermal or otherwise. The observation that radiolarian cherts from other ancient, but more oxygenated marine settings do not tend to retain seawater REE signatures and negative Ce anomalies (Owen et al., 1999) highlights the role that water column anoxia plays in preserving seawater REE distribution patterns in the case of black shales by recycling loosely-bound or soluble REE-phases before deposition.

Braun et al. (2003) report that siliceous radiolarians were an important part of the ocean plankton community by the earliest Cambrian, and were abundant in deeper facies of the Yangtze Platform. Transport to the seafloor was commonly facilitated by the recent arrival of faecal pellets in the Early Cambrian, possibly derived from free-swimming chaetognaths. It is thus entirely plausible that early diagenetic solution of biosiliceous particles was the major source of silicification in black shales as well as black cherts on the Yangtze Platform. At the same time, positive Eu anomalies in some Songtao samples indicate that some of this silica might have derived originally from hydrothermal plumes, a common association during the Palaeozoic (Racki and Cordey, 2000).

Our REE results suggest that hydrogenous silica was also abundant during deposition of the mostly Ediacaran age Liuchapo Formation. In the absence of any evidence for direct precipitation of amorphous silica from seawater (Grenne and Slack, 2003), this indicates that biosiliceous plankton were abundant before the Precambrian–

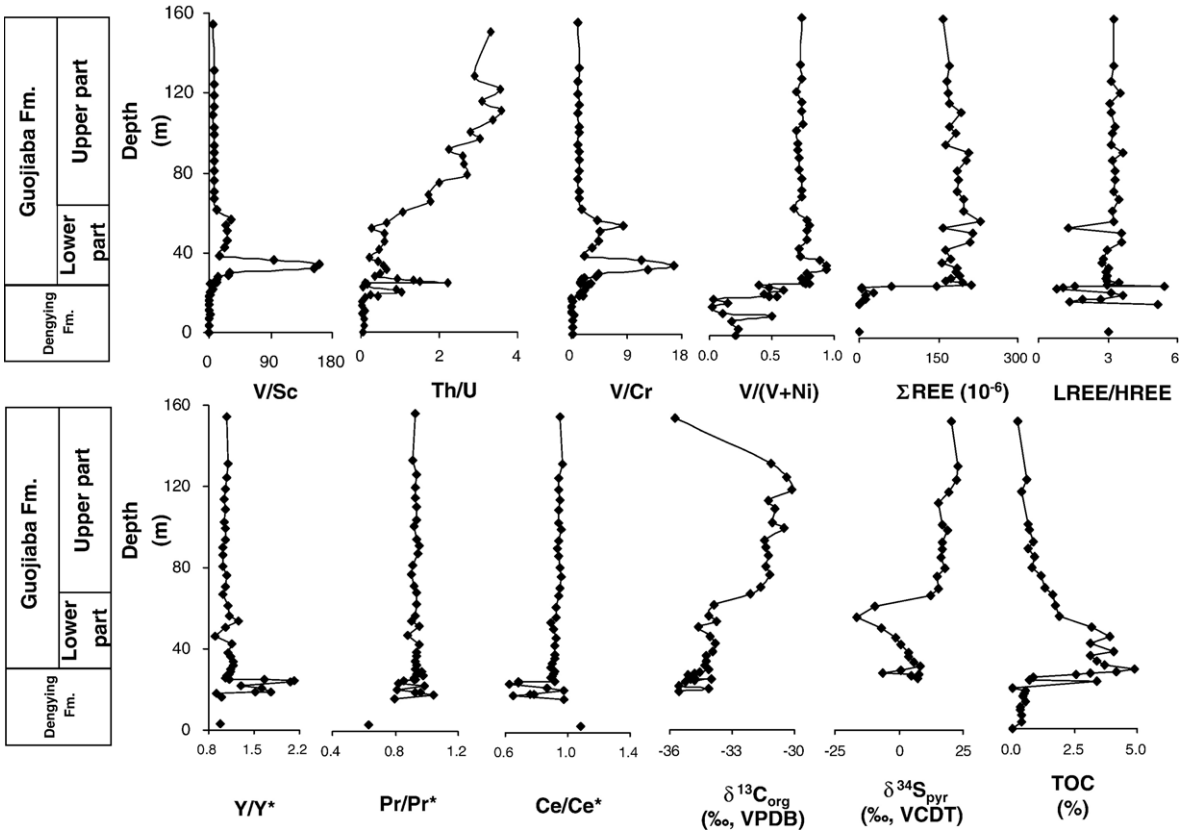

Fig. 12. Stratigraphic distribution of various geochemical parameters in Neoproterozoic–Lower Cambrian sedimentary rocks of the Shatan section, Sichuan Province, South China.

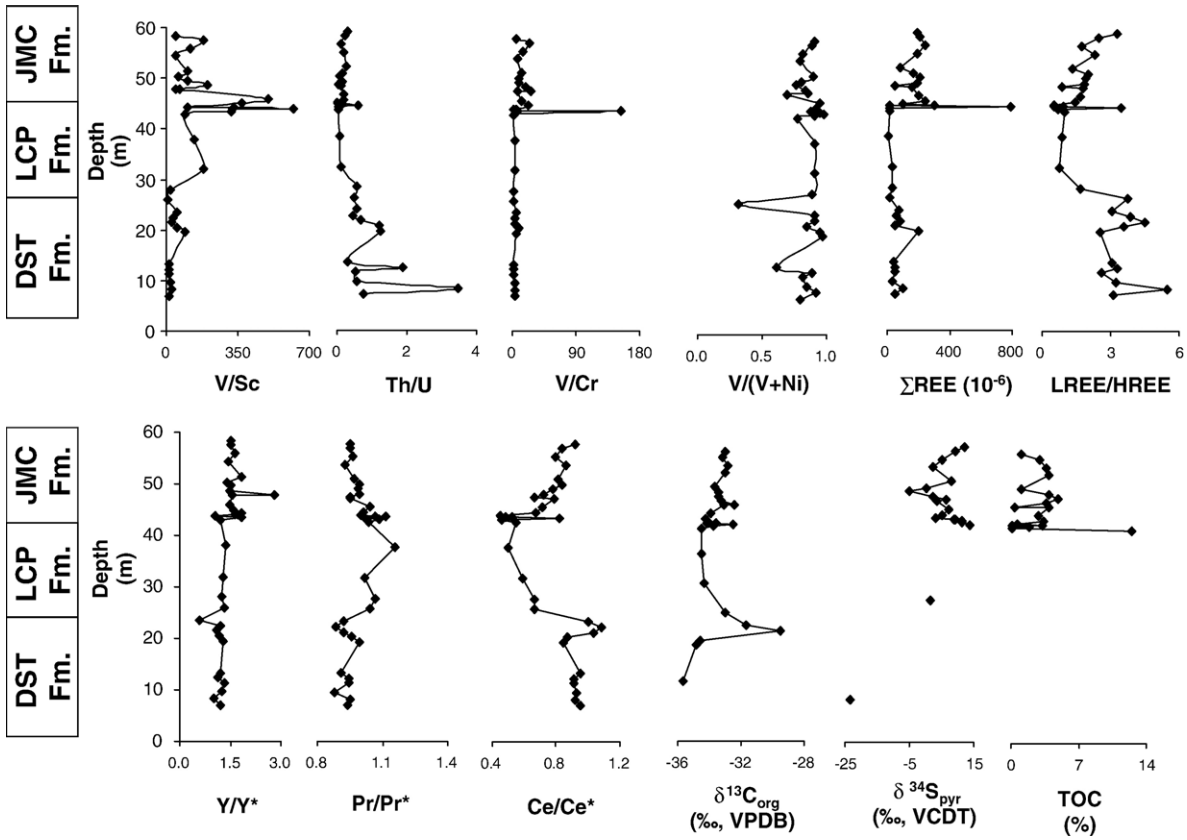

Fig. 13. Stratigraphic distribution of various geochemical parameters in Neoproterozoic–Lower Cambrian sedimentary rocks of the Songtao section, Guizhou Province, South China.

Cambrian boundary. The association of black shales and negative Ce anomalies might act as a geochemical tool for assessing the relative importance of siliceous plankton throughout Earth history (Fig. 13).

6. Conclusions

Across South China, sedimentary strata of Early Cambrian age exhibit characteristic trace metal enrichments in generally organic-rich, stratigraphically correlative, transgressive units. Metal enrichment was widespread from the shelf to the basin and was facilitated by bacterial sulphate reduction, and scavenging of metal sulphides, both within pore waters and directly from bottom waters. Th/U ratios and V/Sc ratios appear to be consistent predictors of anoxia during metal scavenging with Th/U < 0.8, resulting in extreme metal enrichments of V, Ag, Zn and Cd, in particular. Negative Ce anomalies and seawater-like REE distribution patterns are a feature of the Liuchapo chert and lower black shales of the Jiumenchong Formation at Songtao. This unusual REE signature (for shales) is interpreted to derive from biogenic silica that formed from the tests of siliceous phytoplankton, living in the overlying water column. Neither silicification nor hydrothermal fluids, appear to have played a significant role in metal transport. However, hydrothermal plumes from spreading ridge volcanism may have been the initial source of much of the silica and metals.

Acknowledgements

The authors thank all the members of Sino–German Cooperative Program “From Snowball Earth to the Cambrian Bio-radiation: A Multidisciplinary Approach”. Thanks are expressed for assistance and expertise in the field as well as stimulating discussions with Prof. Dr. Jiang Shaoyong, Prof. Chu Xuelei, Prof. Zhang Junming, Prof. Dr. Ling Hongfei, Prof. Feng Hongzhen, Prof. ZhaoYuanlong, Prof. Zhang Qirui, Dr. Yang Aihua et al. Reviews of this manuscript by two anonymous reviewers are also gratefully acknowledged. Support by NSFC (No. 40303001, No. 40672008) and DFG (No. Str 281/16-1/16-2) is gratefully acknowledged.

References

Bau, M., Dulski, P., 1996. Distribution of yttrium and rare-earth elements in the Peng and Kuruman iron-formations, Transvaal Suergroup, South Africa. Precambrian Res. 79, 37–55.

Bowring, S.A., Grotzinger, J.P., Isachsen, C.E., Knoll, A.H., Pelechaty, S.M., Kolosov, P., 1993. Calibrating rates of Early Cambrian evolution. Science 261, 1293–1298.

Braun, A., Chen, J., Maas, A., Waloszek, D., 2003. Plankton from Early Cambrian black shale series on the Yangtze Platform, and its influences on lithologies. Prog. Nat. Sci. 13 (10), 777–782.

Calvert, S.E., Pedersen, T.F., 1993. Geochemistry of Recent oxic and anoxic marine sediments: implications for the geologic record. Mar. Geol. 113, 67–88.

Chen, D., Dong, W., Qi, L., Chen, G., Chen, X., 2003. Possible REE constraints on the depositional and diagenetic environment of Doushantuo Formation phosphorites containing the earliest metazoan fauna. Chem. Geol. 201, 103–111.

Condon, A., Zhu, M., Bowring, S., Wang, W., Yang, A., Jin, Y., 2005. U–Pb Ages from the Neoproterozoic Doushantuo Formation, China. Science 308, 95–98.

Cruse, A.M., Lyons, T.W., 2004. Trace metal records of regional paleoenvironmental variability in Pennsylvanian (Upper Carboniferous) black shales. Chem. Geol. 206, 319–345.

Douville, E., Bienvenu, P., Charlou, J.L., Donval, J.P., Fouquet, Y., Appriou, P., Gamo, T., 1999. Yttrium and rare earth elements in fluids from various deep-sea hydrothermal systems. Geochim. Cosmochim. Acta 63, 627.

Drever, J.T., 1988. Geochemical cycles: the continental crust and the oceans. In: Gregor, C.B. (Ed.), Chemical Cycles. John Wiley, New York, pp. 17–53.

Fan, D., 1984. The Lower Cambrian black series and the iridium anomaly in south China. Developments in Geosciences. Contribution to 27th International Geological Congress, Moscow. Science Press, pp. 215–224.

Goldberg, T., Strauss, H., Guo, Q., Liu, C., 2007. Reconstructing marine redox conditions for the Early Cambrian Yangtze Platform: evidence from biogenic sulphur and organic carbon isotopes. Palaeogeogr. Palaeoclimatol. Palaeoecol. 254, 56–88 (this volume) , doi:10.1016/j.palaeo.2007.03.015.

Gradstein, F.M., Ogg, J.G., Smith, A.G., 2005. A Geologic Time Scale 2004. Cambridge University Press0521786738.

Grenne, T., Slack, J.F., 2003. Paleozoic and Mesozoic silica-rich seawater: Evidence from hematitic chert (jasper) deposits. Geology 31, 319–322.

Guo, Q., Liu, C., Strauss, H., Goldberg, T., 2003. Isotopic evolution of the terminal Neoproterozoic and early Cambrian carbon cycle on the northern Yangtze Platform, South China. Prog. Nat. Sci. 13 (12), 942–945.

Guo, Q., Strauss, H., Liu, C., Goldberg, T., Zhu, M., Heubeck, C., Pi, D., Vernhet, E., Yang, X., Fu, P., 2007. Carbon isotopic evolution of the terminal Neoproterozoic and Early Cambrian: evidence from the Yangtze Platform, South China. Palaeogeography, Palaeoclimatology, Palaeoecology 254, 137–154 (this volume), doi:10.1016/j.palaeo.2007.03.014.

He, Y., Yang, X., 1986. Coelenterate fossils of the early-Early Cambrian from Nanjiang, Sichuan Province, China (in Chinese) Chengdu Institute of geological Mineral deposits publication. CAGS, vol. 7, pp. 31–48.

Holser, W.T., 1997. Evaluation of the application of rare-earth elements to paleoceanography. Palaeogeogr. Palaeoclimatol. Palaeoecol. 132, 309–323.

Kimura, H., Watanabe, Y., 2001. Ocean anoxia at the Precambrian–Cambrian boundary. Geology 29, 995–998.

Li, S., Gao, Z., 1995. REE characteristics of black rock series of the Lower Cambrian Niutitang Formation in Hunan–Guizhou Provinces, China, with a discussion on the REE patterns in marine hydrothermal sediments. Acta Min. Sin. 15 (2), 225–229 (in Chinese with English abstract).

Li, S., Gao, Z., 1996. Silicalite of hydrothermal origin in the Lower Cambrian black rock series of South China. Acta Min. Sin. 16 (4), 416–422 (in Chinese with English abstract).

Liu, Y., Chao, L., Li, Z., Wang, H., Chu, T., Zhang, J., 1984. Trace Elements Geochemistry. Science Press, Beijing, pp. 1–548 (in Chinese).

Lott, D.A., Coveney Jr., R.M., Murowchick, J.B., Grauch, R.I., 1999. Sedimentary exhalative Nickel–Molybdenum ores in south China. Econ. Geol. 94, 1051–1066.

Mao, J., Lehmann, B., Du, A., Zhang, G., Ma, D., Wang, Y., Zeng, M., Kerrich, R., 2002. Re–Os dating of polymetallic Ni–Mo–PGE–Au mineralization in Lower Cambrian black shales of South China and its geologic significance. Econ. Geol. 97, 1051–1061.

Mclennan, S.M., 1989. Rare earth elements in sedimentary rocks: Influence of provenance and sedimentary processes. Rev. Miner. 21, 169–200.

Mclennan, S.M., 2001. Relationships between the trace element composition of sedimentary rocks and upper continental crust. Geochem. Geophys. Geosyst. 2 (2000GC000109).

Michard, A., Albarède, F., 1986. The REE content of some hydrothermal fluids. Chem. Geol. 55, 51–60.

Murray, R.W., Buchholtz ten Brink, M.R., Gerlach, D.C., Russ, G.P., Jones, D.L., 1991. Rare earth, major, and trace elements in chert from the Franciscan Complex and Monterey Group, California: Assessing REE sources to fine-grained marine sediments. Geochim. Cosmochim. Acta 55, 1875–1895.

Olivarez, A.M., Owen, R.M., 1991. The europium anomaly of seawater: implications for fluvial versus hydrothermal REE inputs to the oceans. Chem. Geol. 92, 317–328.

Owen, A.W., Armstrong, H.A., Floyd, J.D., 1999. Rare earth element geochemistry of upper Ordovician cherts from the Southern Upland of Scotland. J. Geol. Soc. 156, 191–204.

Pan, J., Ma, D., Cao, S., 2004. Trace element geochemistry of the Lower Cambrian black rock series from northwestern Hunan, South China. Prog. Nat. Sci. August 85–91.

Racki, G., Cordey, F., 2000. Radiolaria palaeoecology and radiolarites: Is the present the key to the past? Earth-Sci. Rev. 52, 83–120.

Rimmer, S.M., 2004. Geochemical paleoredox indicators in Devonian–Mississippian black shales, Central Appalachian Basin (USA). Chem. Geol. 206, 373–391.

Rogers, J.J.W., Adams, J.A.S., 1976. Handbook of Thorium and Uranium Geochemistry. Atomic Press, Beijing. (Chinese version).

Ruhlin, D.E., et al., 1986. The rare earth element geochemistry of hydrothermal sediments from the East Pacific Rise: examination of a seawater scavenging mechanism. Geochim. Cosmochim. Acta 50, 393.

Shields, G., Stille, P., 2001. Diagenetic constraints on the use of cerium anomalies as palaeoseawater redox proxies: an isotopic and REE study of Cambrian phosphorites. Chem. Geol. 175, 29–48.

Shields, G., Stille, P., Brasier, M.D., Atudorei, N.V., 1997. Stratified oceans and oxygenation of the late Proterozoic environment: a post glacial geochemical record from the Neoproterozoic of W Mongolia. Terra Nova 9, 218–222.

Steiner, M., Wallis, E., Erdtmann, B.D., Zhao, Y., Yang, R., 2001. Submarine–hydrothermal exhalative ore layers in black shales from South China and associated fossils — insights into a Lower

Cambrian facies and bio-evolution. Palaeogeogr. Palaeoclimatol. Palaeoecol. 169, 165–191.

Steiner, M., Li, G., Qi, Y., Zhu, M., 2004. Lower Cambrian small shelly fossils of northern Shaanxi (China), and their biostratigraphic importance. Geobios 37, 259–275.

Torres, M.E., Bohrmann, G., Dub´e, T.E., Poole, F.G., 2003. Formation of modern and Paleozoic barite at continental margin methane seeps. Geology 31, 897–900.

Wedepohl, K.H., Correns, C.W., Shaw, D.W., Turekian, K.K., Zemann, J., 1978. Handbook of Geochemistry, vol.1-11(1–5). Springer-Verlag, New York.

Wignall, P.B., Twitchett, R.J., 1996. Oceanic anoxia and the end Permian mass extinction. Science 272, 1155–1158.

Wilde, P., Quinby-Hunt, M.S., Erdtmann, B.D., 1996. The whole-rock cerium anomaly: a potential indicator of eustatic sea-level changes in shales of the anoxic facies. Sediment. Geol. 101, 43–53.

Wilde, P., Lyons, T.W., Quinby-Hunt, M.S., 2004. Organic carbon proxies in black shales: molybdenum. Chem. Geol. 206, 167–176.

Yang, X.H., He, Y., 1984. New small shelly fossils genera of the Lower Cambrian from Nanjiang, Sichuan Province, China. Strata and Palaeotology Papers Assemblage, vol. 13, pp. 35–47 (in Chinese).

Yang, X., He, Y., Deng, S., 1983. Precambrian–Cambrian Boundary and Small Shelly Fossils Fauna from Nanjiang, Sichuan Province, China. Chengdu Institute of Geological Mineral Deposits Publication, vol. 4. CAGS, pp. 91–110 (in Chinese).

Yang, A., Zhu, M., Zhang, J., Li, G., 2003. Early Cambrian eodiscoid trilobites of the Yangtze Platform and their stratigraphic implications. Prog. Nat. Sci. 13 (12), 861–866.

Zhu, M., Zhang, J., Steiner, M., Yang, A., 2003. Sinian–Cambrian stratigraphic framework for shallow- to deep-water environments of the Yangtze Platform: an integrated approach. Prog. Nat. Sci. 13 (12), 951–960.